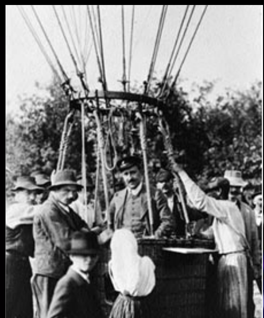

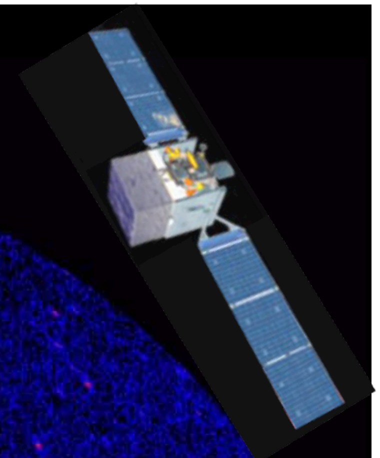

DECIPHERING THE MILKY WAY WITH GALPROP

IGOR V MOSKALENKO – STANFORD

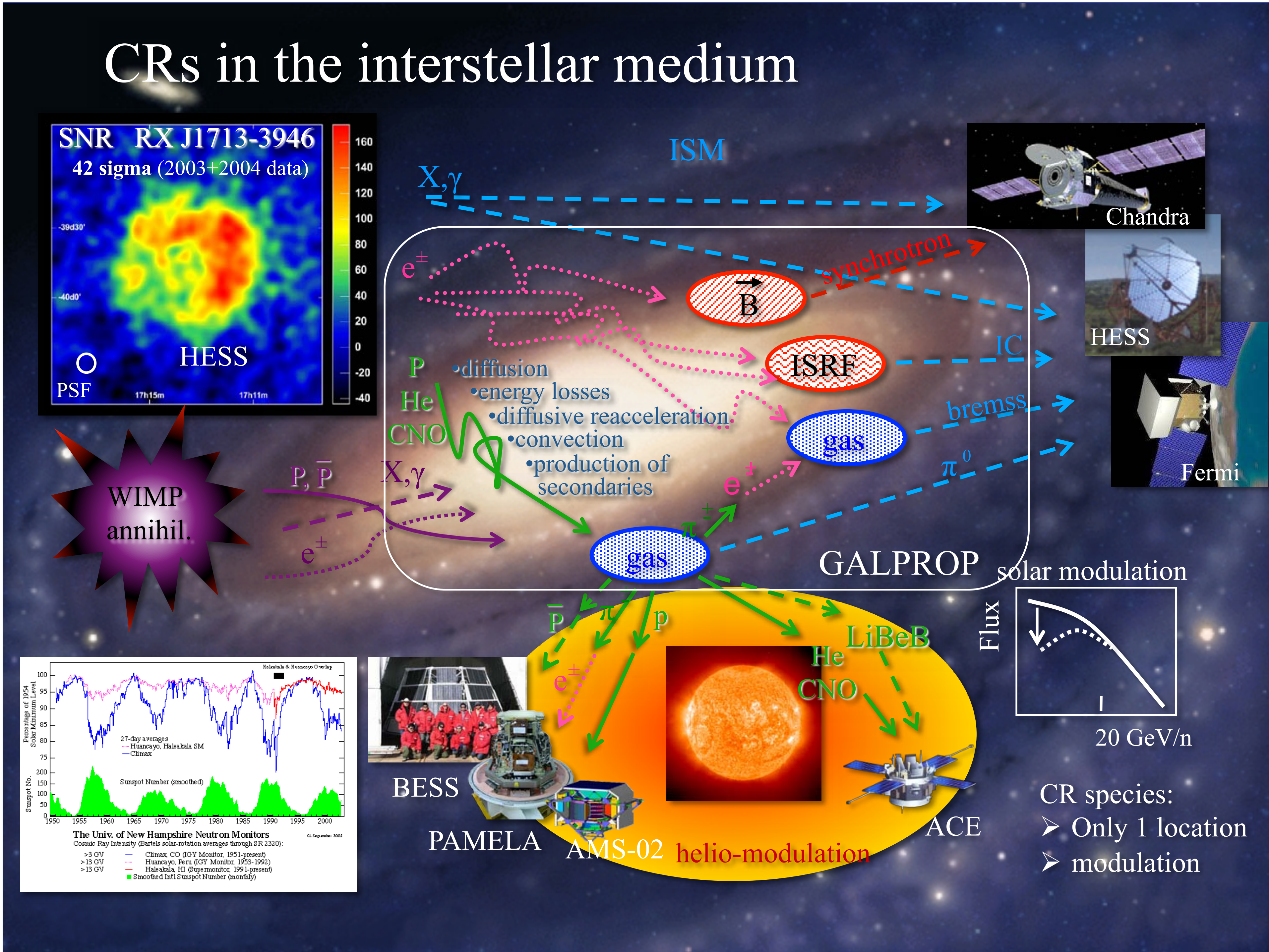
CRs in the interstellar medium
SNR RX J1713-3946
42 sigma (2003+2004 data)
HESS
PSF
ISM
X,γ
Chandra
HESS
Fermi
synchrotron
B
ISRF
IC
gas
bremss
π0
e±
P
He
CNO
•diffusion
•energy losses
•diffusive reacceleration
•convection
•production of secondaries
WIMP annihil.
P, P̄
X,γ
e±
gas
π±
GALPROP
solar modulation
Flux
20 GeV/n
P̄
π
p
LiBeB
He
CNO
e±
BESS
PAMELA
AMS-02
helio-modulation
ACE
The Univ. of New Hampshire Neutron Monitors
CR species:
➢ Only 1 location
➢ modulation

High energy gamma-ray emission processes

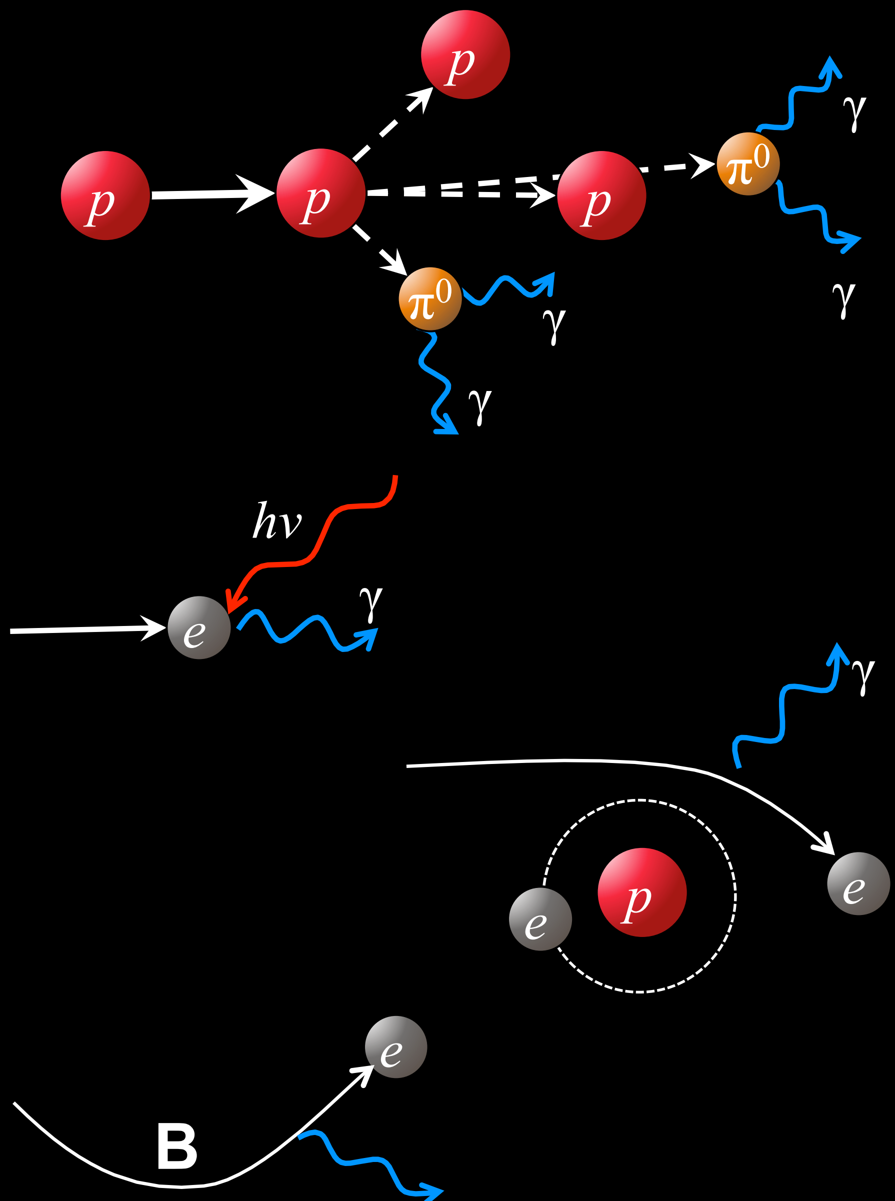

- ✧ $pp \rightarrow \pi^0(2\gamma)+X$ – neutral pion production and decay
- ✧ Inverse Compton scattering
- ✧ Bremsstrahlung
- ✧ Curvature (or synchrotron) radiation

Inner Galaxy at different wavelengths

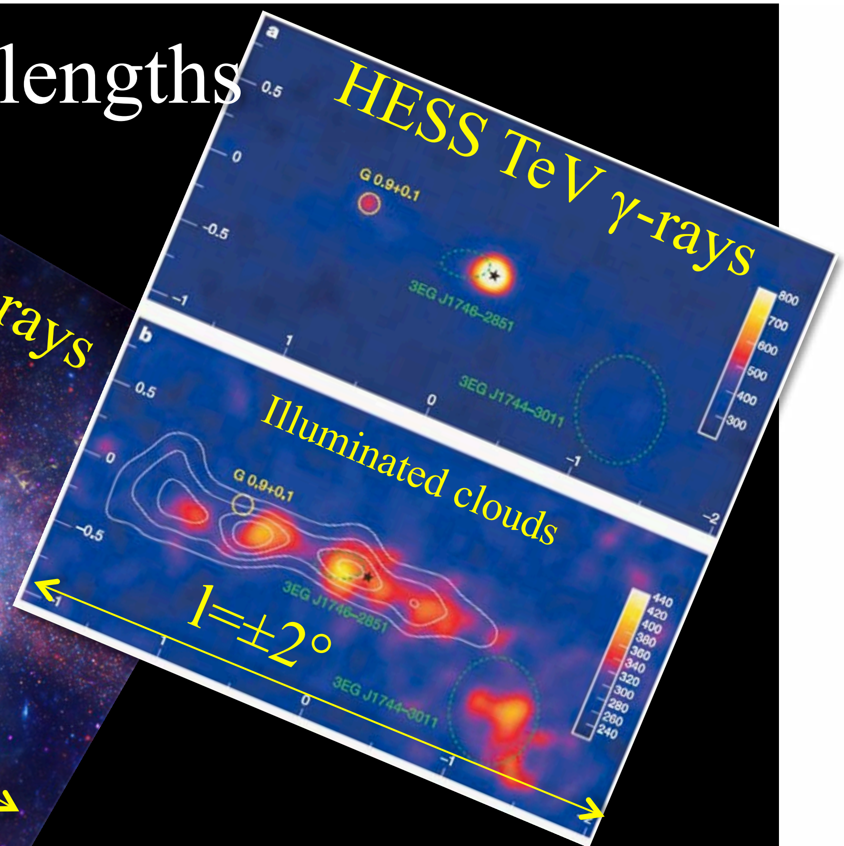

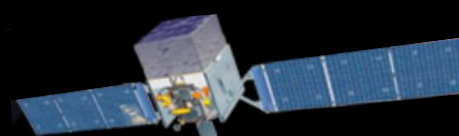

✧ Continuous collection of data by the Fermi-LAT significantly adds to the available multi-λ data

What is in the inner Galaxy?

- ✧ Harbors a SMBH ~4×10^6 $M_\odot$
- ✧ Flaring activity of SMBH: large flare ~100 years ago, and faint flares
- ✧ Huge over-density of dark matter
- ✧ 1000s of stars in the innermost parsec
- ✧ Large concentration of binary systems and compact objects
- ✧ "Paradox of youth" – old (?) stars look like young
- ✧ "Fermi Bubbles" (Finkbeiner+'2010)

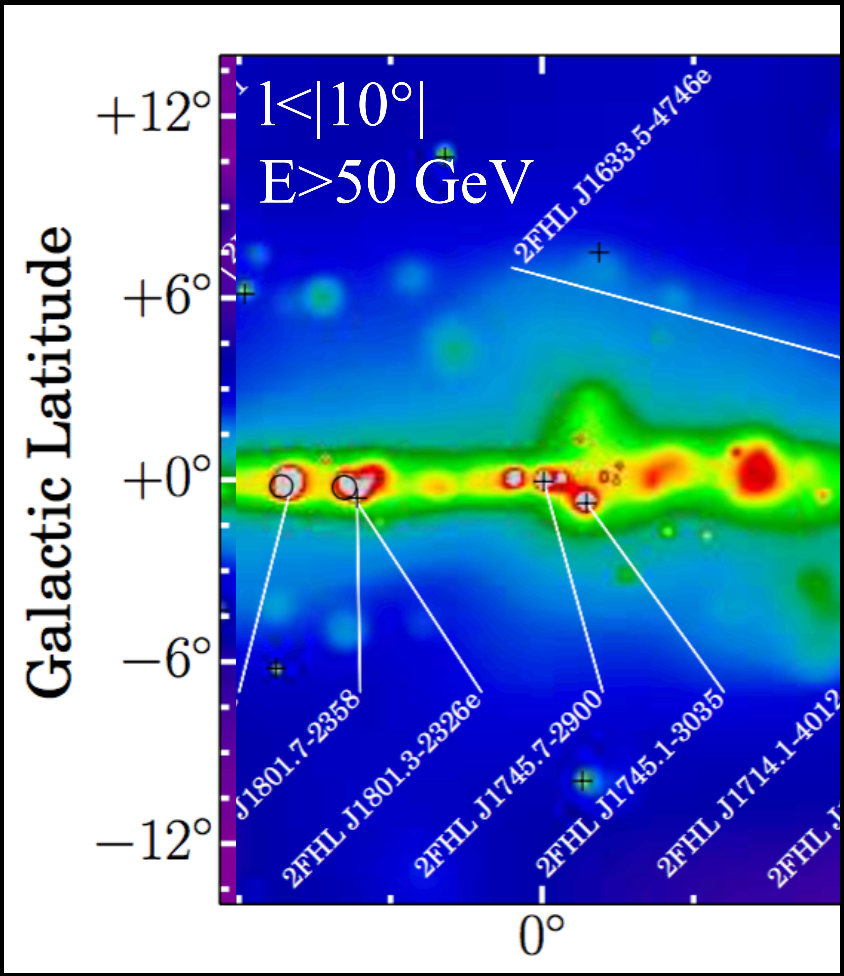

- ✧ Guaranteed new physics results!

Fermi-LAT: Ajello+'2016

Fermi-LAT Study of the Inner Galaxy

Scaling Procedure

- Determine intensity for π^0 (from HI and H_2 gas) and IC contributions in galactocentric rings,
  - IC component divided in rings (dev. version of GALPROP), same boundaries as the gas: these additional degrees of freedom can compensate for uncertainies in the GALPROP model of the electron spectrum or ISRF used to calculate the IC templates
- Isotropic and Loop I (*Wolleben, 2007, ApJ 664*) emissions also fitted to the data
- Different sky regions are employed based on where the components that are fitted dominate. Point source locations and spectra taken from the preliminary 3FGL.

Galactocentric ring boundaries.

Ring #	R_{min} [kpc]	R_{max} [kpc]	Longitude Range (Full)
1	0	1.5	$-10° \leq l \leq 10°$
2	1.5	2.5	$-17° \leq l \leq 17°$
3	2.5	3.5	$-24° \leq l \leq 24°$
4	3.5	8.0	$-70° \leq l \leq 70°$
5	8.0	10.0	$-180 \leq l \leq 180°$
6	10.0	50.0	$-180 \leq l \leq 180°$

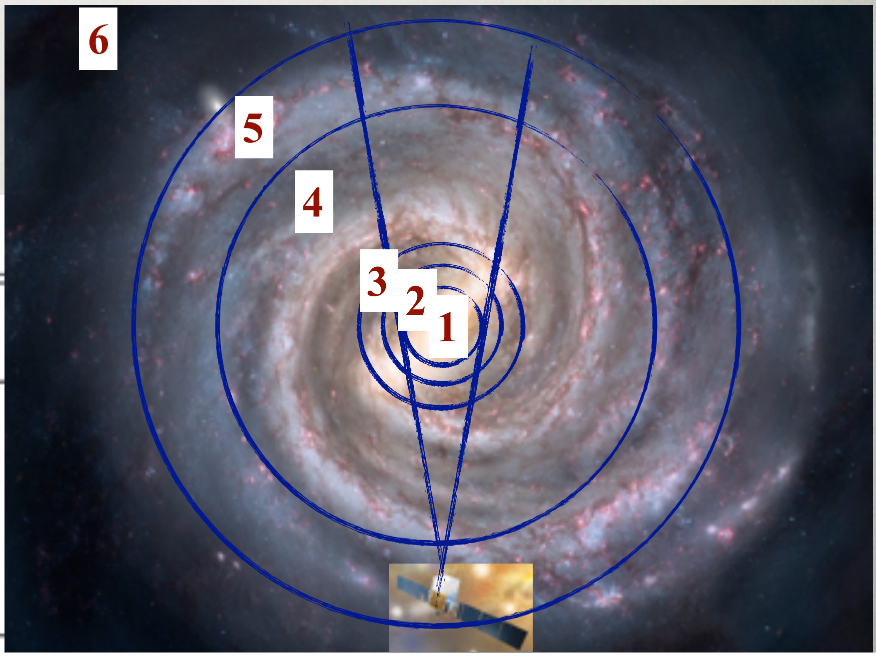

Sources in the inner Galaxy

- ✧ PGWave – candidate sources
- ✧ Fixing the background model allows the sources to be detected
- ✧ The sources' position and spectra depend on the background model – looping back
- ✧ The brightest sources (TS≥25) are not very much model-dependent

● – 1FIG sources TS≥25

× – 1FIG source candidates TS≤25

+ – 3FGL sources with multi-wavelengths associations

(1FIG = 1st Fermi Inner Galaxy Catalog)

Fermi-LAT: Ajello+'2016

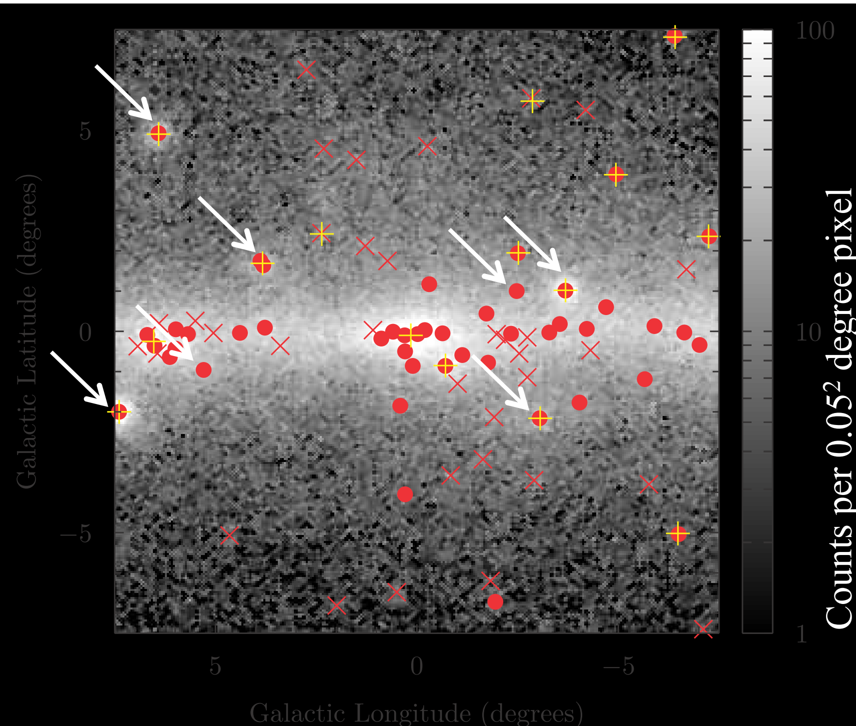

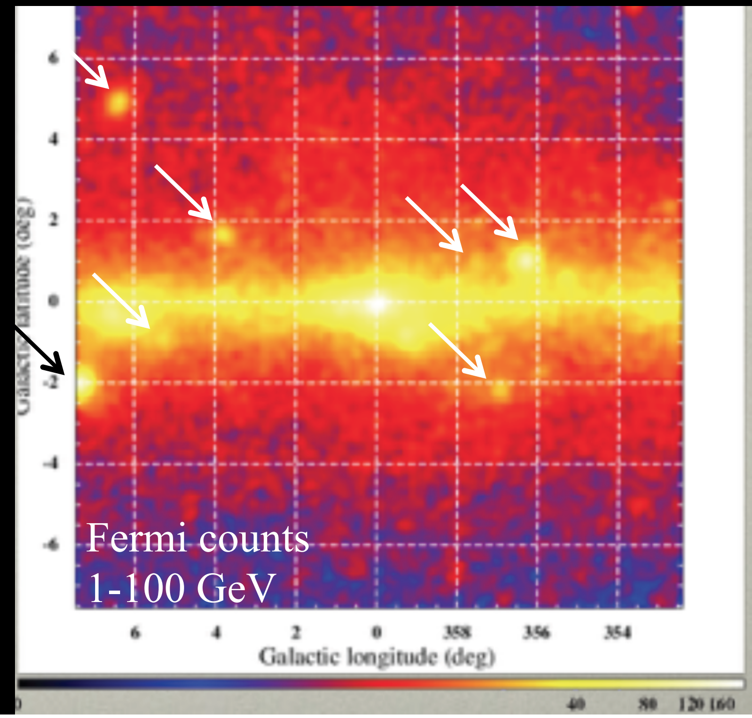

Fermi-LAT: Ajello+'2016

Point sources removed

Results - Residual Maps

DATA-MODEL

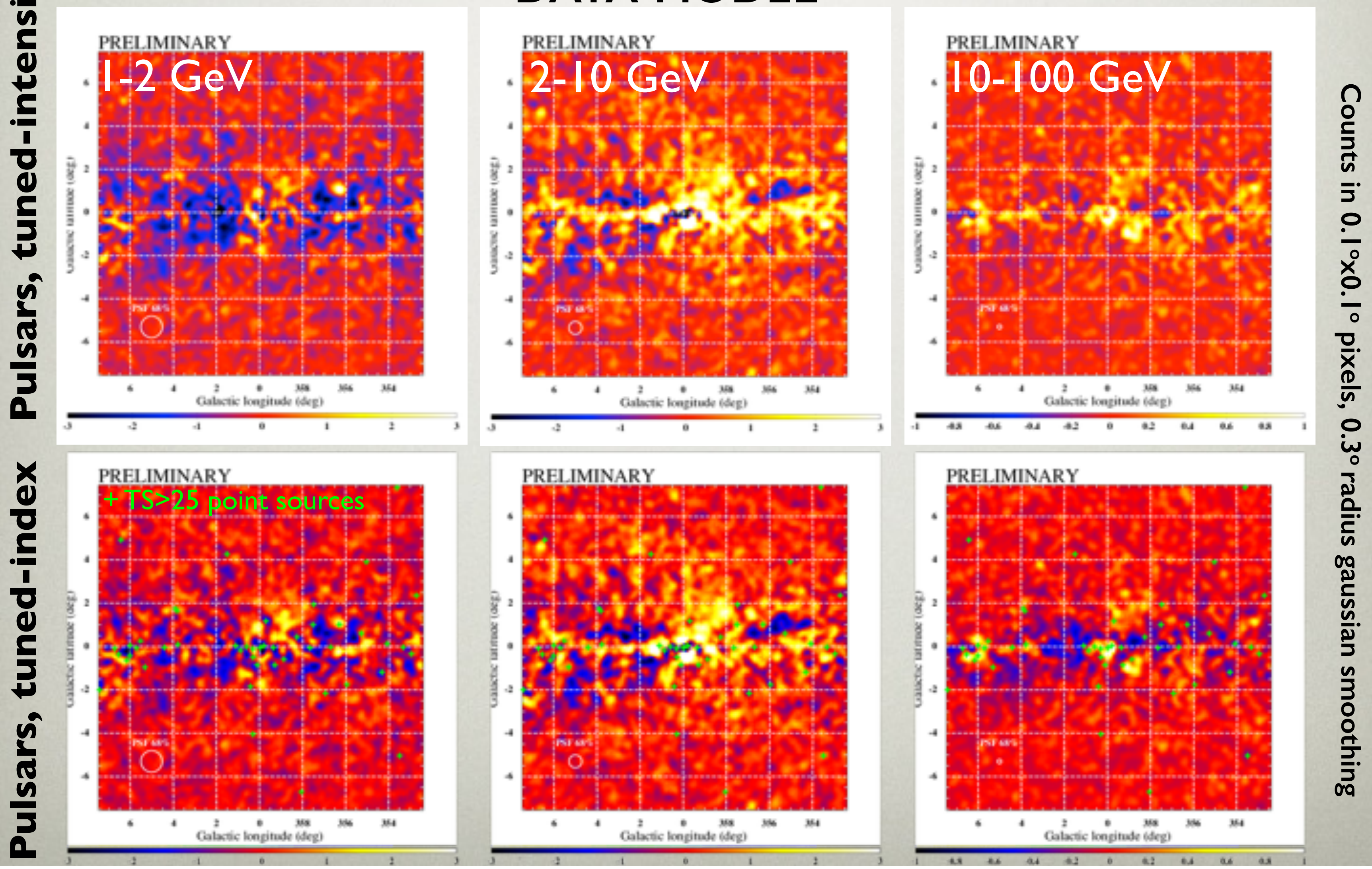

Fermi-LAT: Ajello+’2016

Results - Dark Matter

DATA-MODEL (Pulsars, index scaled)

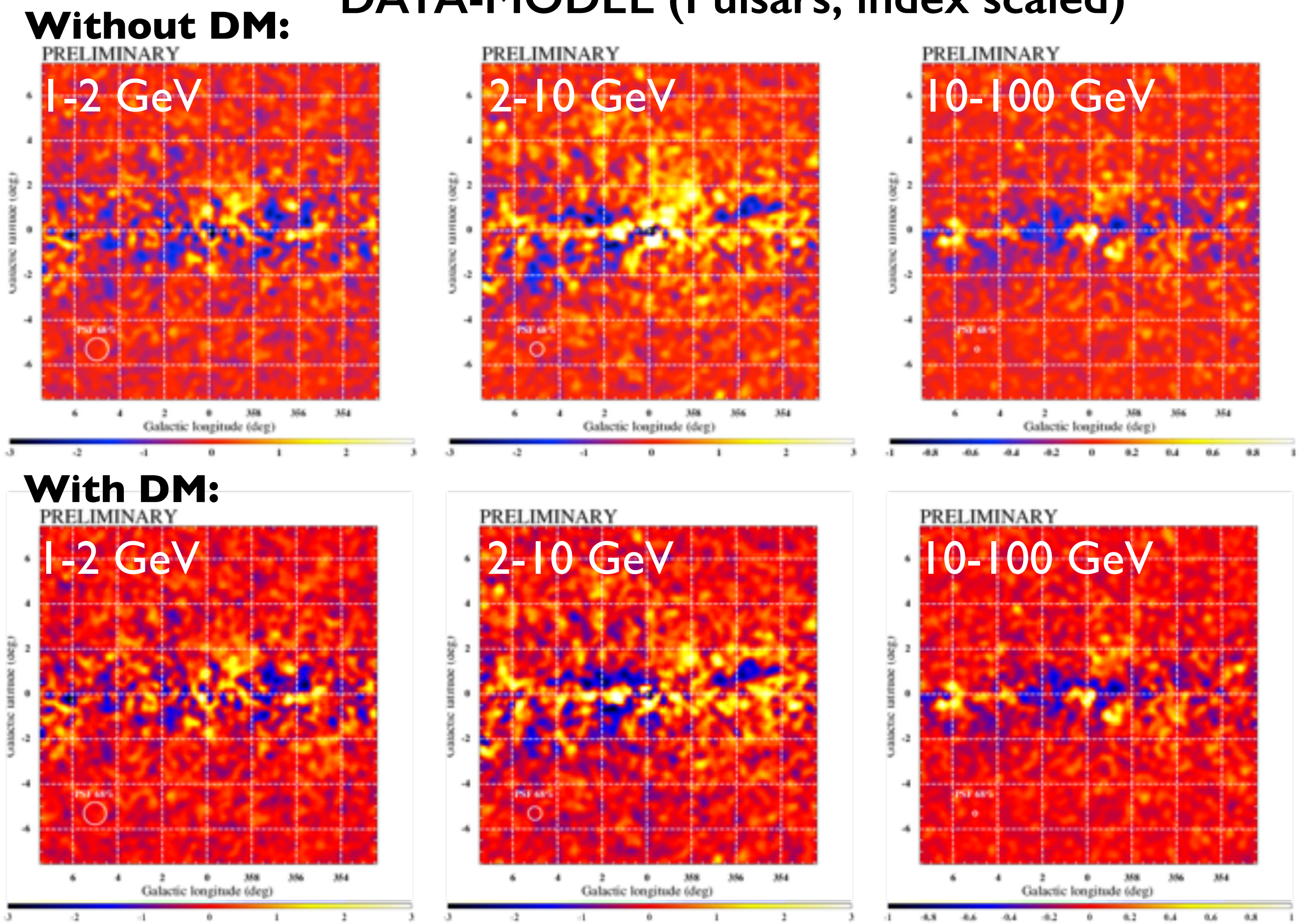

Counts in 0.1°x0.1° pixels, 0.3° radius gaussian smoothing

Fermi-LAT: Ajello+'2016

- ✦ There is a positive residual in the 15°x15° region which persists for all IEMs we used
- ✦ A DM template improves the agreement with the data and its spectral properties vary widely depending on the IEM, however:
  - Some discrepancies remain and might be due to mismodeling of the IEM
  - There are limitations in the IEMs, e.g. the gas distribution, cylindrical symmetry, as well as interplay between the interstellar emission and point sources.

    Understanding these issues is crucial to confirm the presence and properties of additional components, DM or otherwise

With DM:

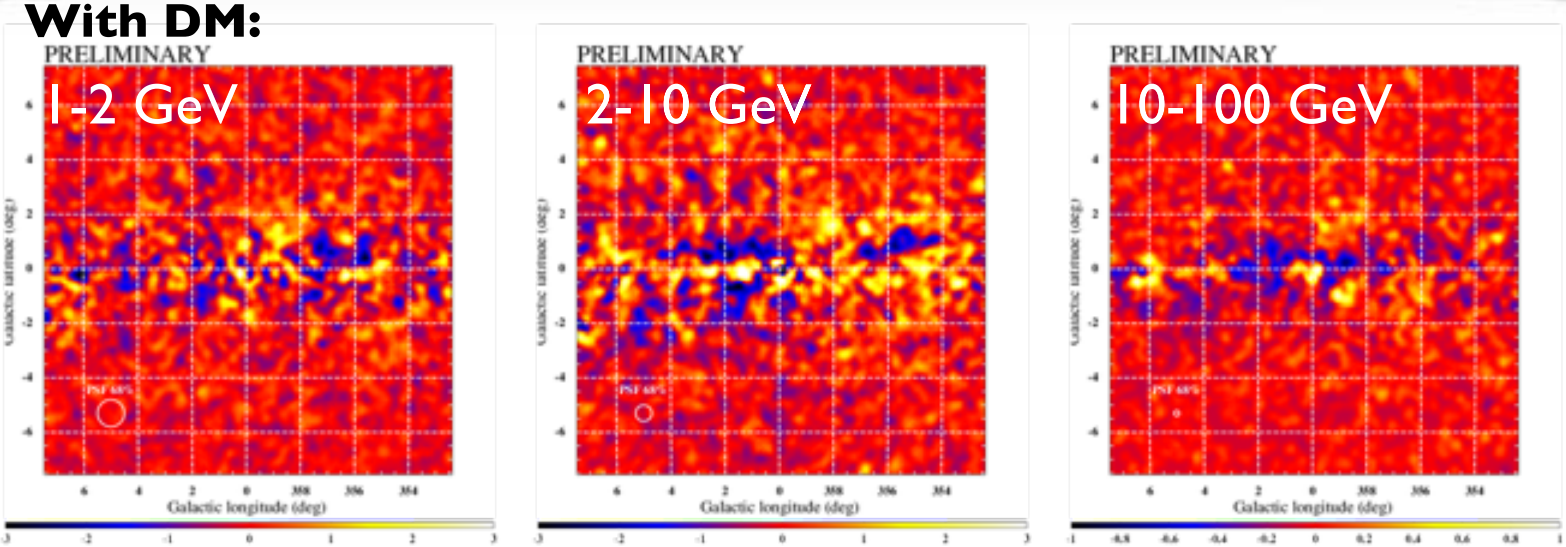

0.3° radius gaussian smoothing

NFW component in different background models

- ✧ A peaked NFW profile

$$\rho(r) = \frac{\rho_0}{\frac{r}{R_s}\left(1 + \frac{r}{R_s}\right)^2}$$

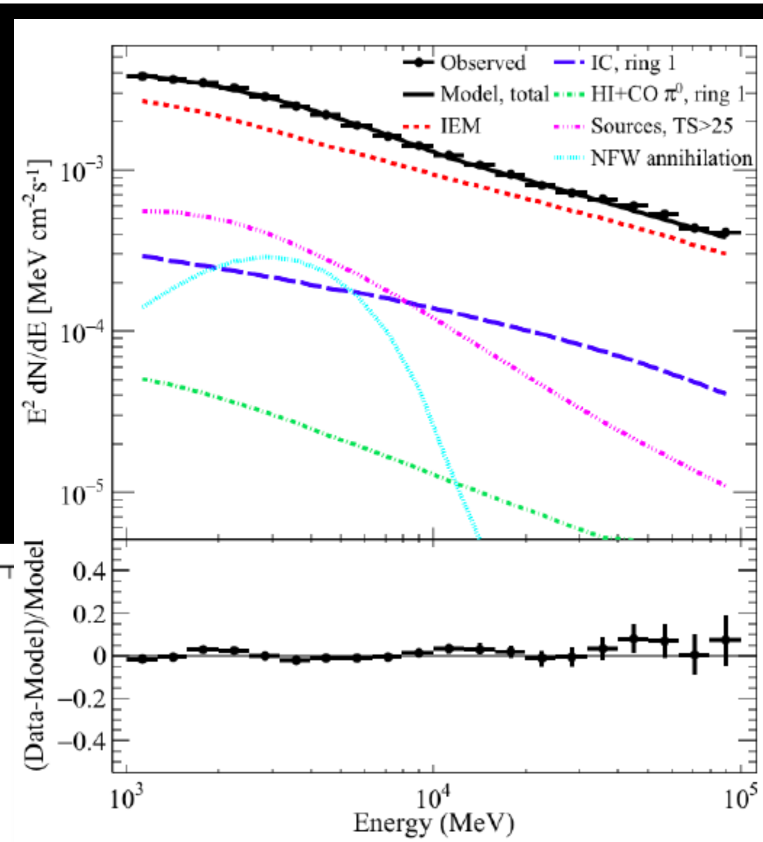

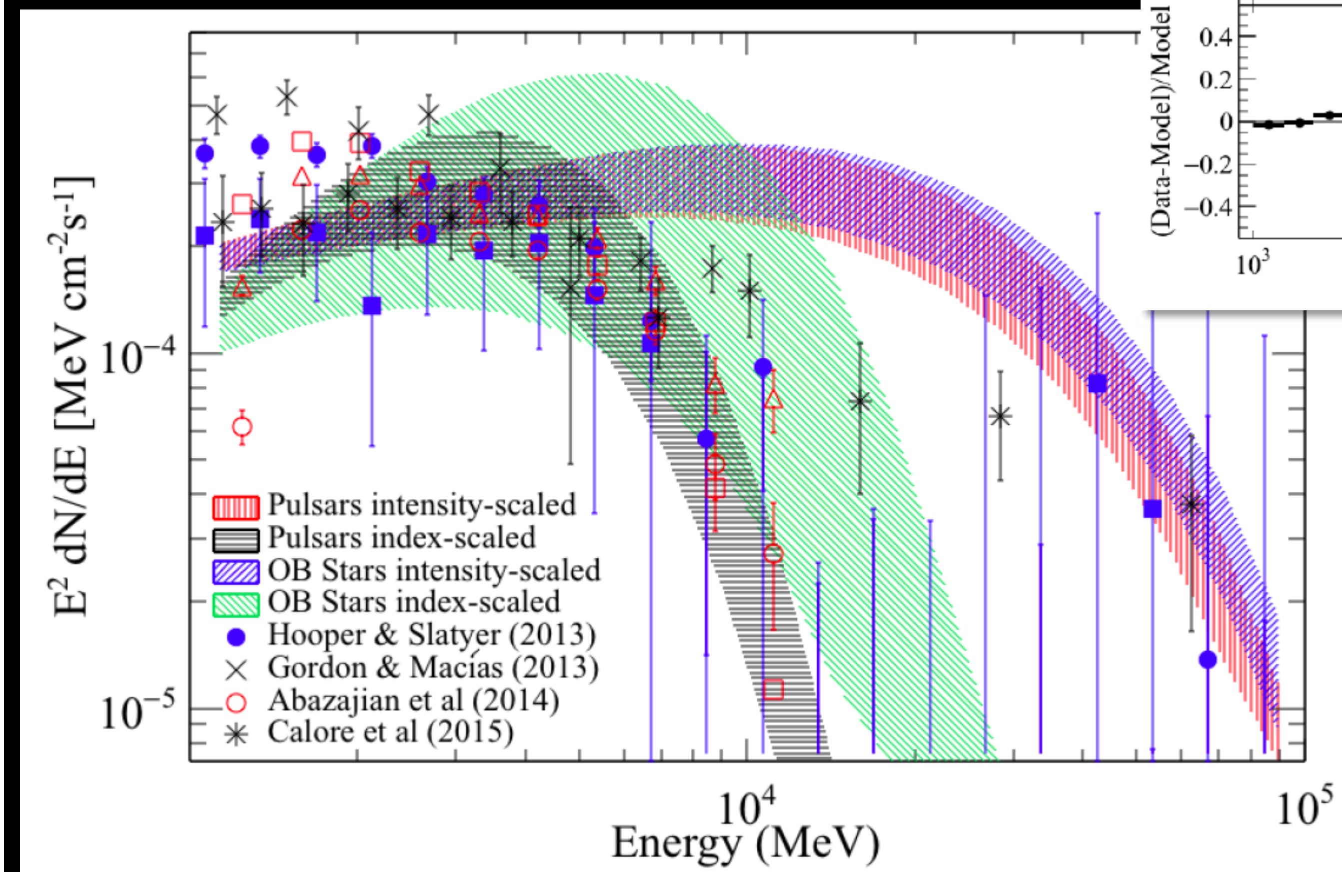

- ✧ Components of the emission observed in the inner 15°×15° (one of the models)
- ✧ Spectrum of the NFW component in different models

Voyager 1 in the interstellar space

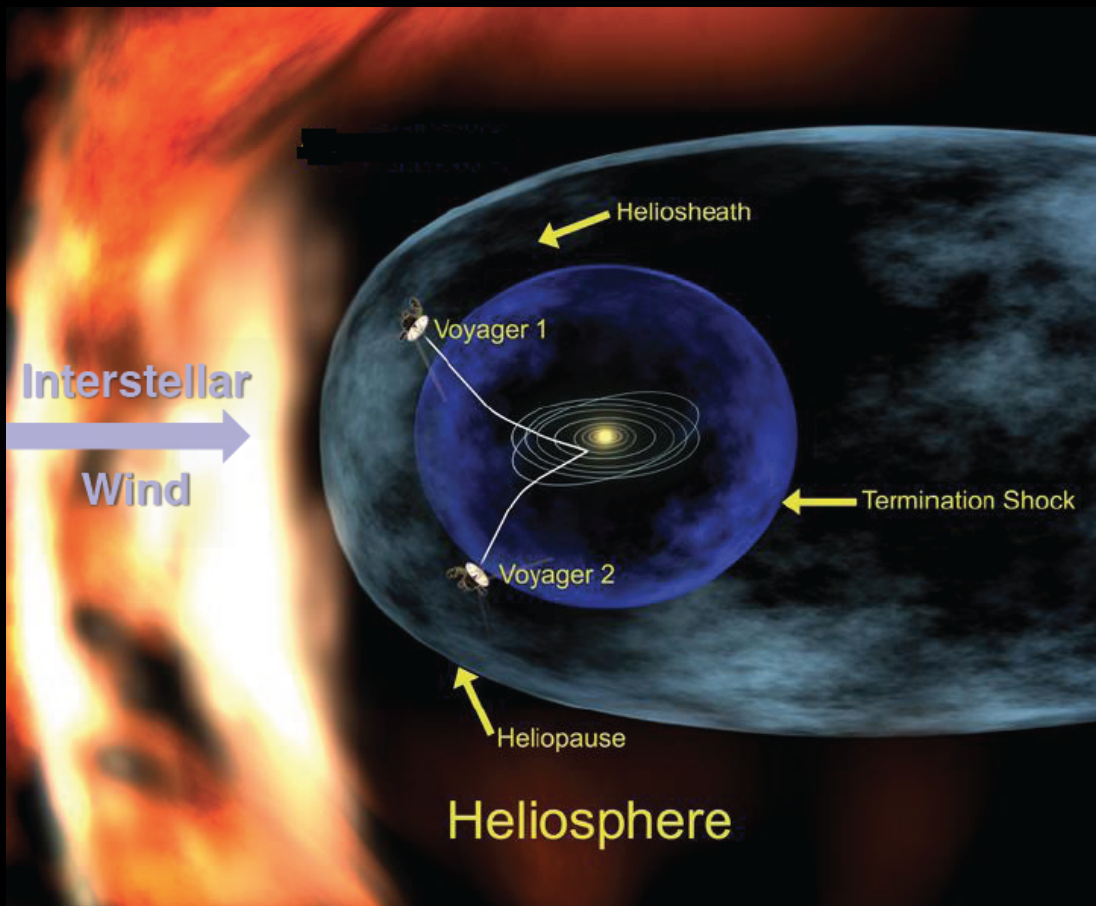

Voyager 1 131.0 AU
19.7 billion km

Voyager 2   107.7 AU
16.2 billion km
~2 years to interstellar space?

Launched in 1977!

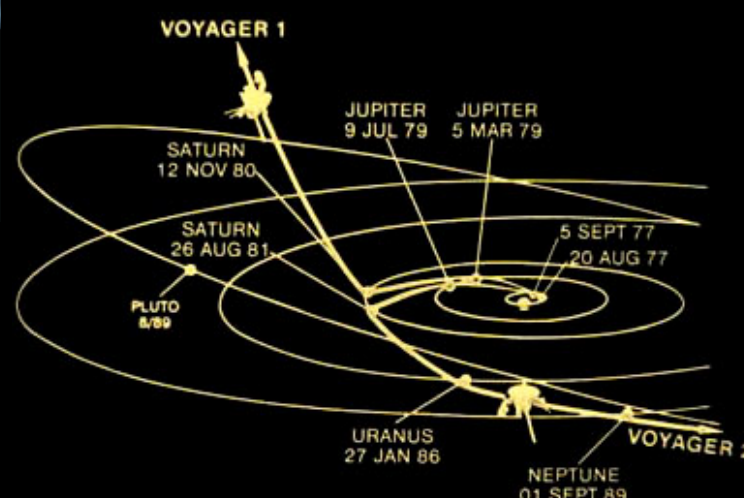

First interstellar probe!
Will operate until 2026

E. Stone 2015

Cosmic ray fluxes in the heliosphere

- CR flux along the Voyager 1 path
- Note some delay relative to the sunspot maxima
- Weak last solar max helps – smaller size of the heliosphere

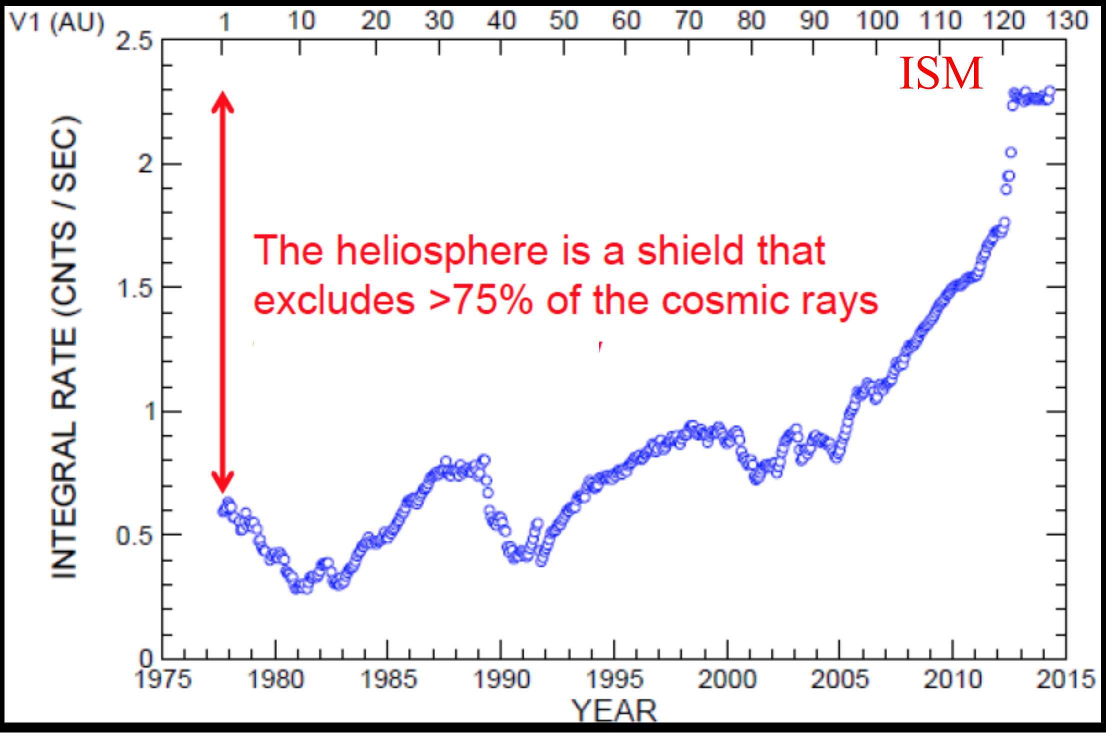

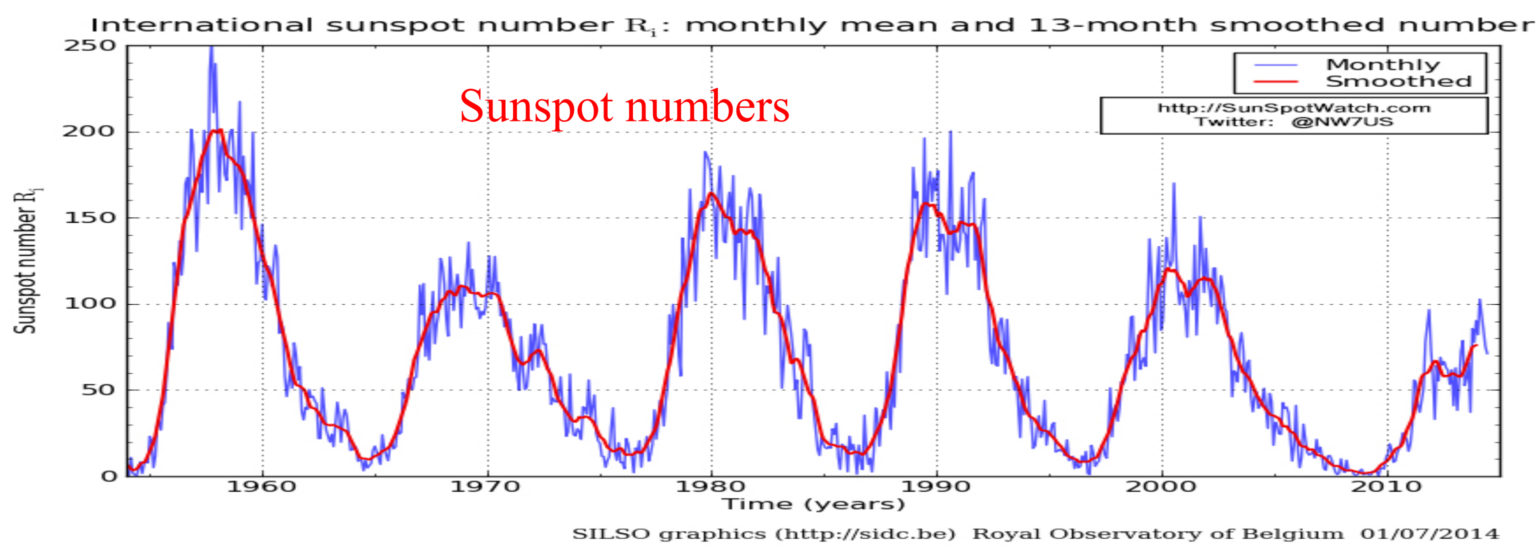

Interstellar probe – Voyager 1

(A) (y axis on right) GCR nuclei (E > 70 MeV) at the High Energy Telescope 1

(B) (y axis on left) GCR electrons (6-100 MeV) observed by the Electron Telescope

(C) (y axis on left) Protons with 7 to 60 MeV stopping in HET 1 are mainly anomalous cosmic rays before 2012/238 (25 August) and galactic cosmic rays after that

(D) (y axis on left) Low-energy particles mainly protons with 0.5 to ~30 MeV accelerated at the termination shock and in the heliosheath

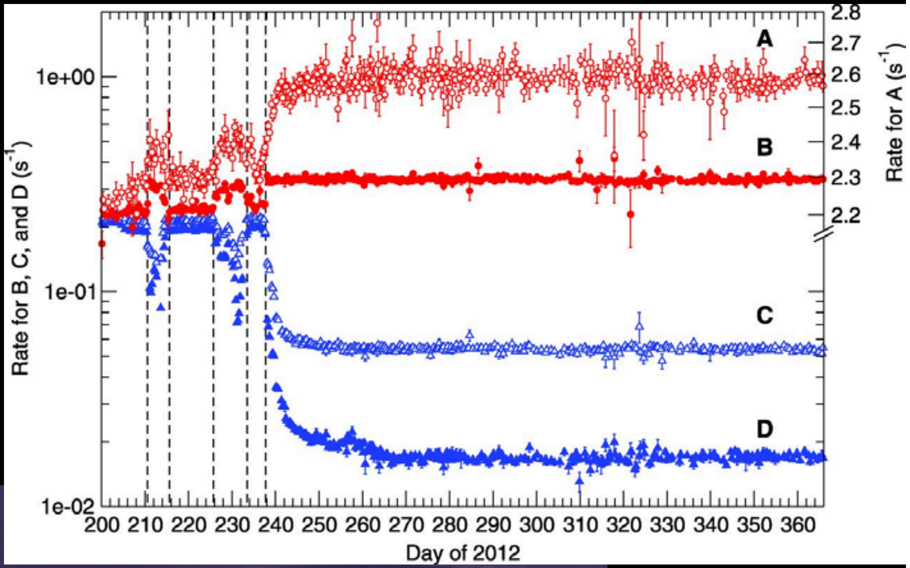

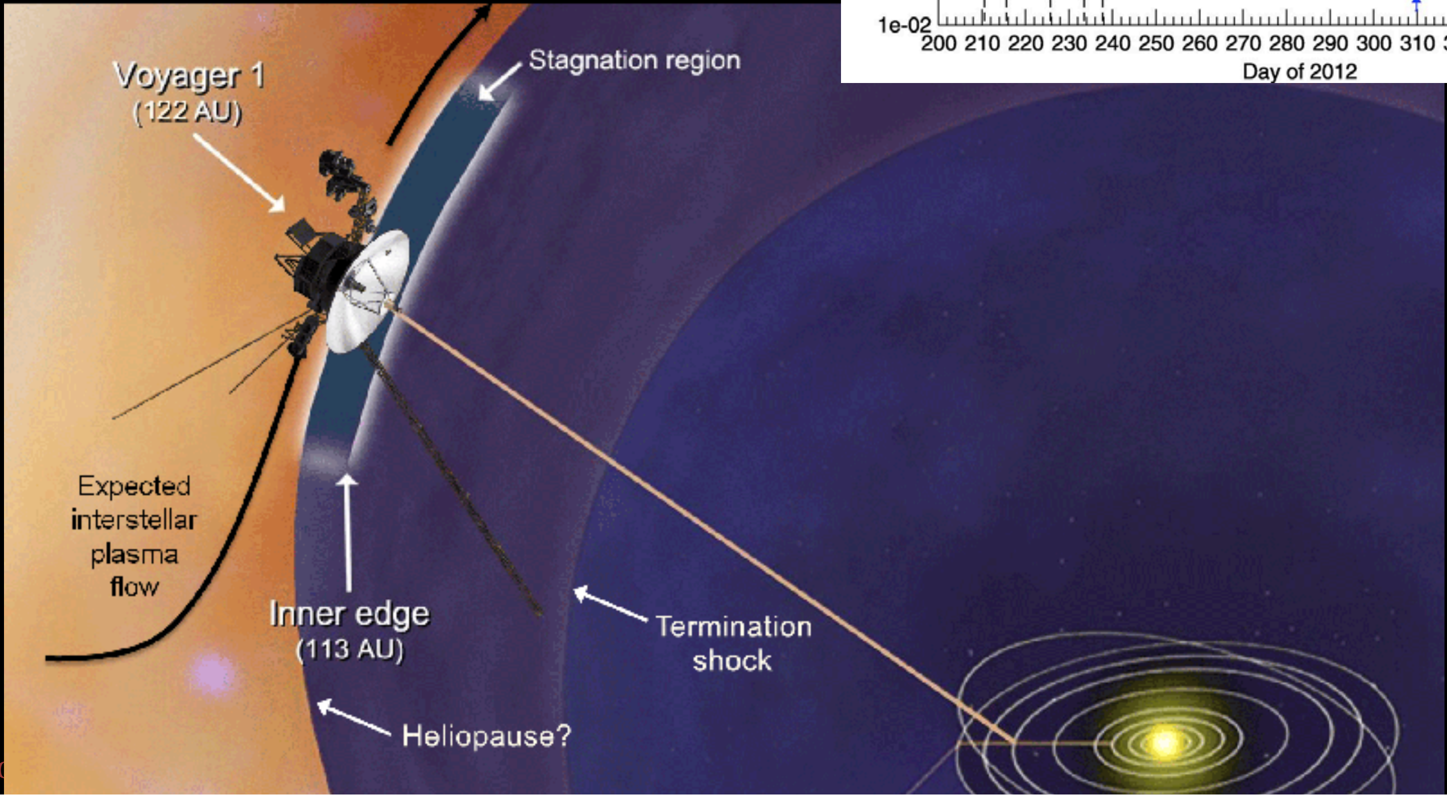

Voyager 1 spectra for 2012/342-2014/365

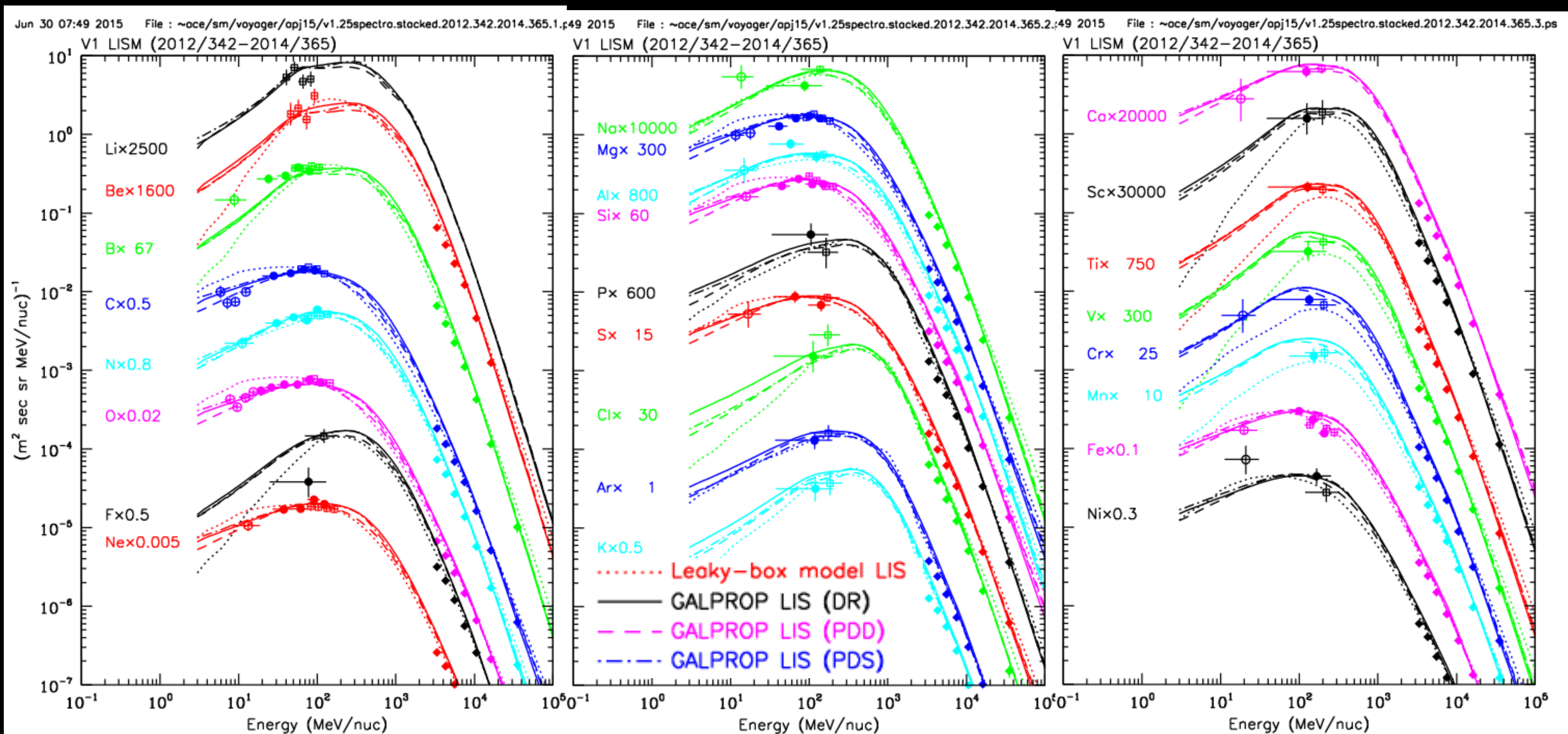

Li – Ni : V1 spectra together with HEAO-3-C2 data (≥3.35 GeV/nuc)

Cummings+’2016

Voyager 1 – H and He spectra

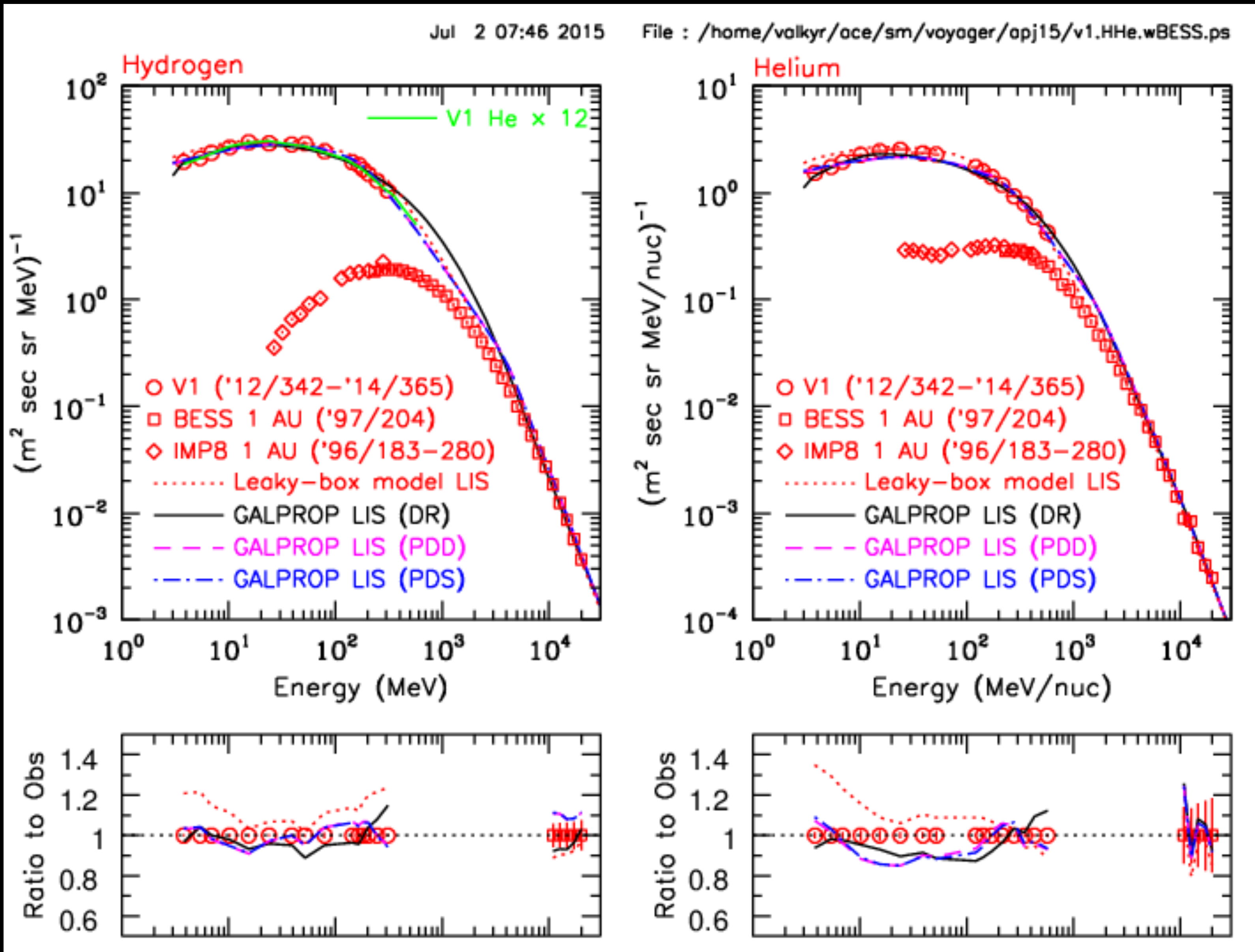

Cummings+'2016

Energy losses of nucleons

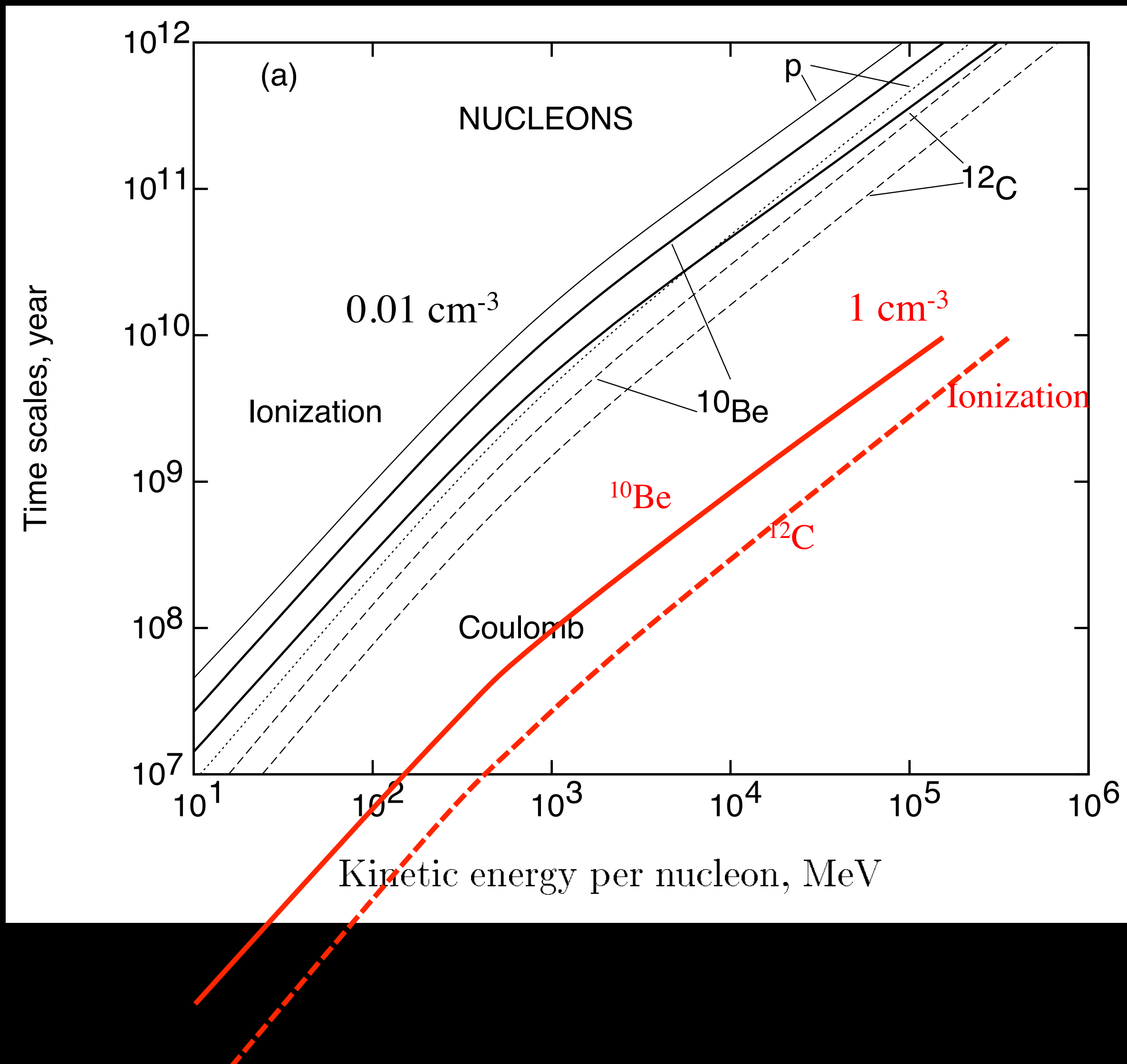

- The ionization and Coulomb losses are calculated for the gas number density 0.01 cm^{-3} & 1 cm^{-3}

  Carbon at 10 MeV/n (nH ~1 cm^{-3}):

  $\tau \sim 30$ kyr
- Important conclusion – no close source of low energy cosmic rays
- The energy losses by nucleons can be neglected above ~1 GeV
- Nuclear interactions are more important

Heliospheric Propagation – what is it all about?

- ✧ Propagation of CRs through the heliosphere ~130 AU – a minuscule distance by the Galactic scale, posed a considerable challenge until now
- ✧ These last 0.0006 pc are so important – provide a link between the predictions of the interstellar propagation models with the location where 99.9% of all direct CR measurements are made
- ✧ Even though, the heliospheric modulation affects only spectra below 30–50 GeV, this range includes the sub-GeV energies where the most precise measurements of CR isotopic composition are made
- ✧ Low energy data are used to derive the parameters of interstellar propagation that are then extrapolated onto the whole Galaxy and all energies up to the multi-TeV region
- ✧ An improvement in the description of the heliospheric propagation has a global impact on our understanding of CR phenomena in the whole Galaxy

Charge-sign effect

The Parker magnetic field has opposite magnetic polarity above and below the helio-equator, but the spiral field lines are mirror images of each other.

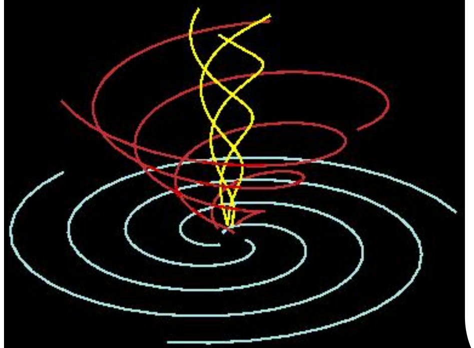

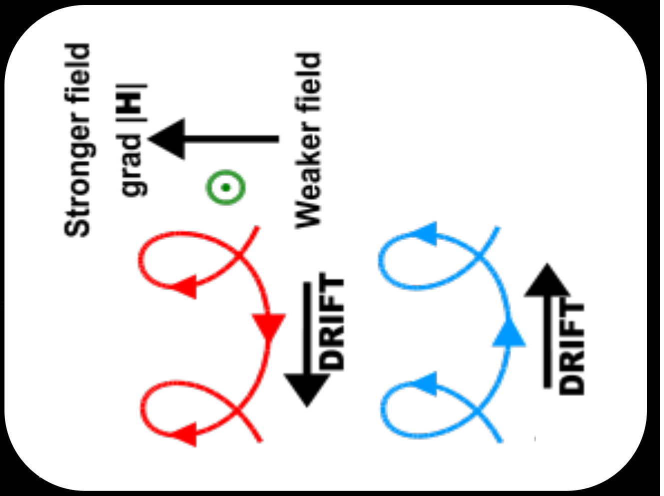

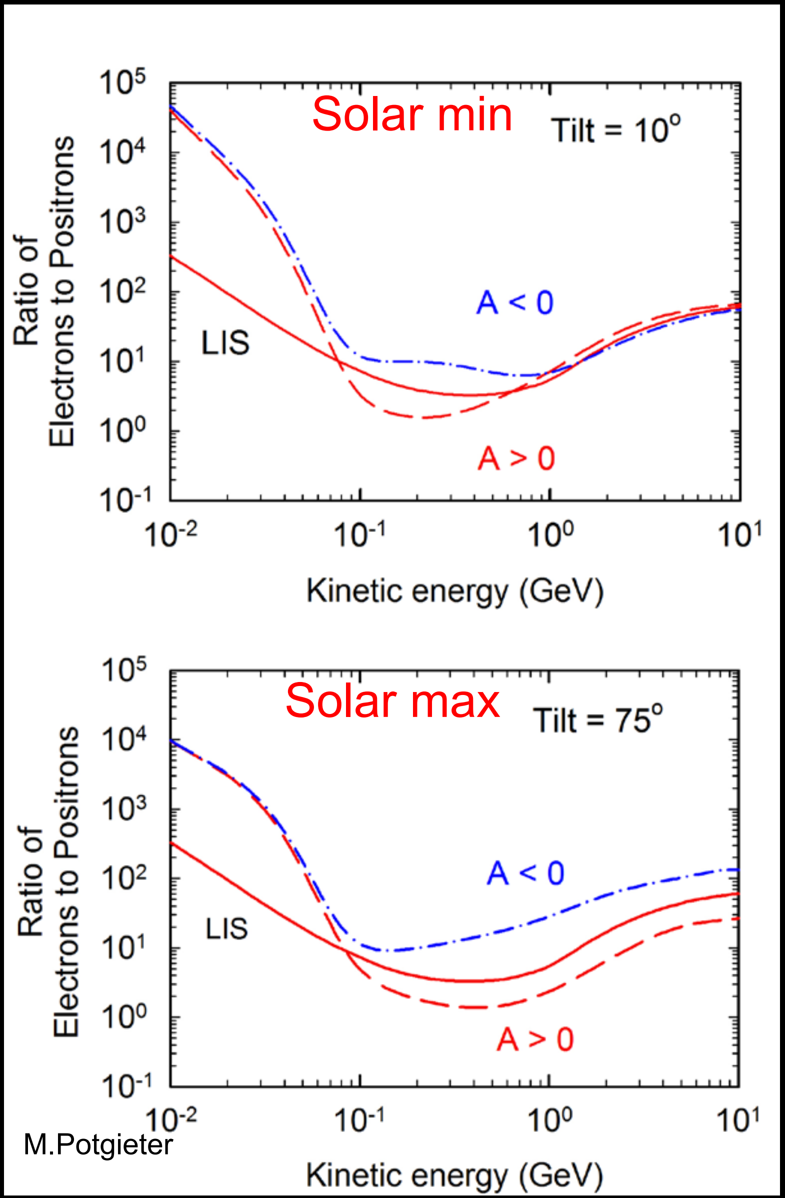

This antisymmetry produces the drift velocity fields that affect the particles of opposite charge in different ways (converge on heliospheric equator or diverge from it).

Charge-sign effect: Positron fraction'2015

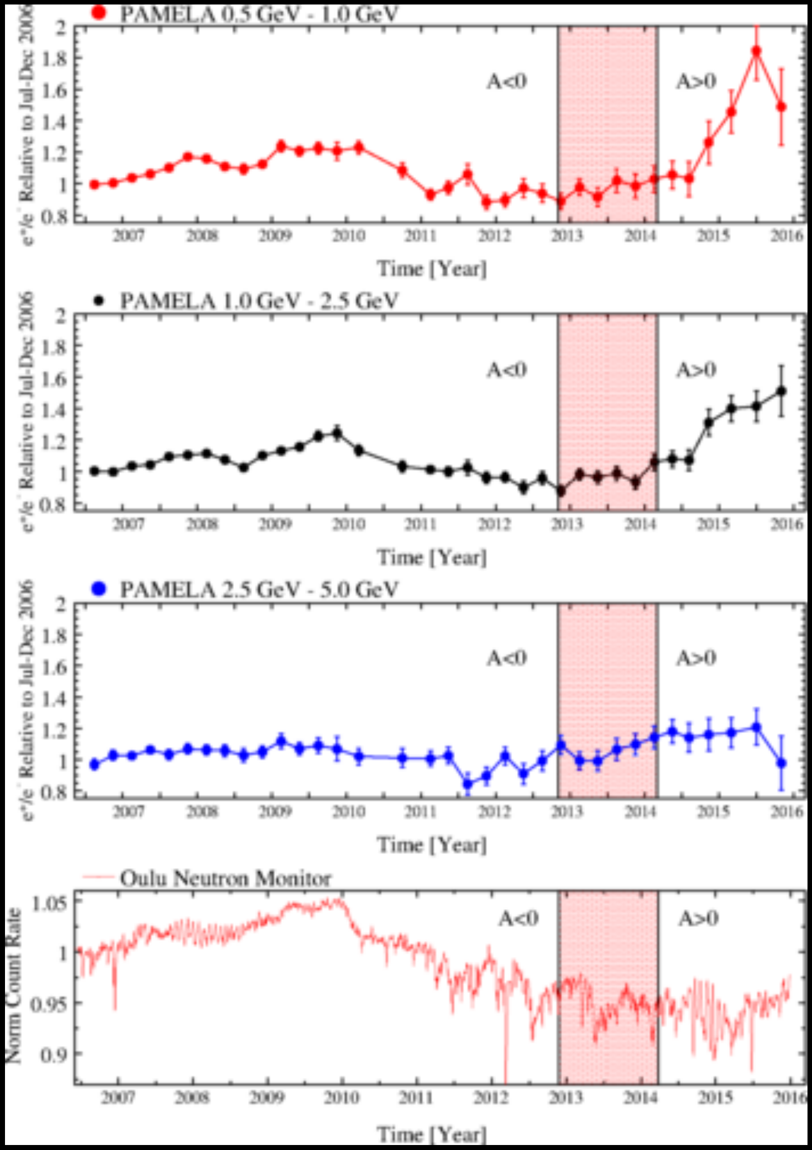

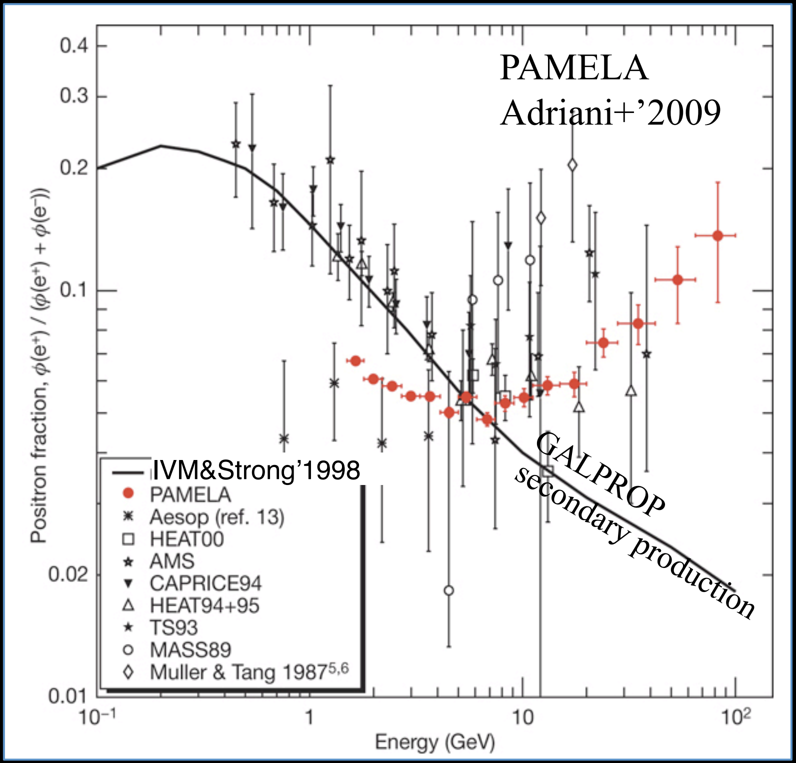

PAMELA – Adriani+'2016

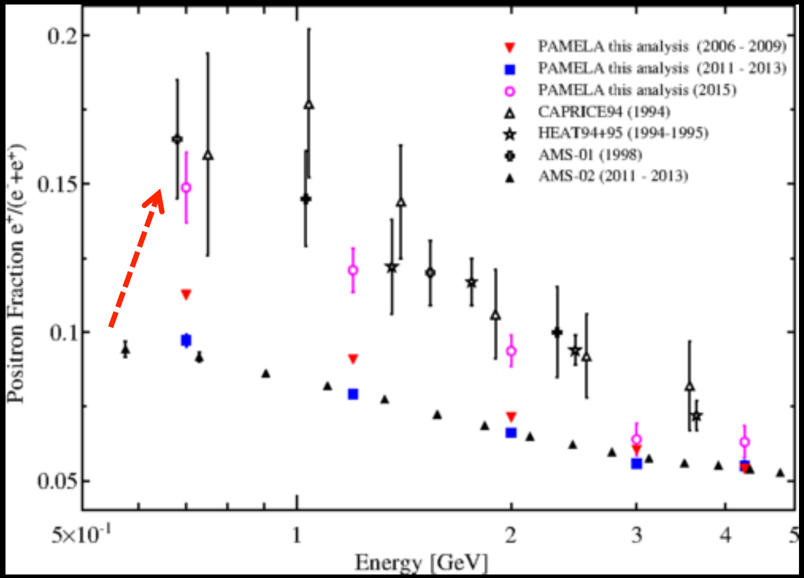

HELMOD

- ✧ GALPROP/HelMod – paper in progress
- ✧ Goal: reliable spectra of CR species in the interstellar medium (>100 MeV/n) and modulation for arbitrary epoch

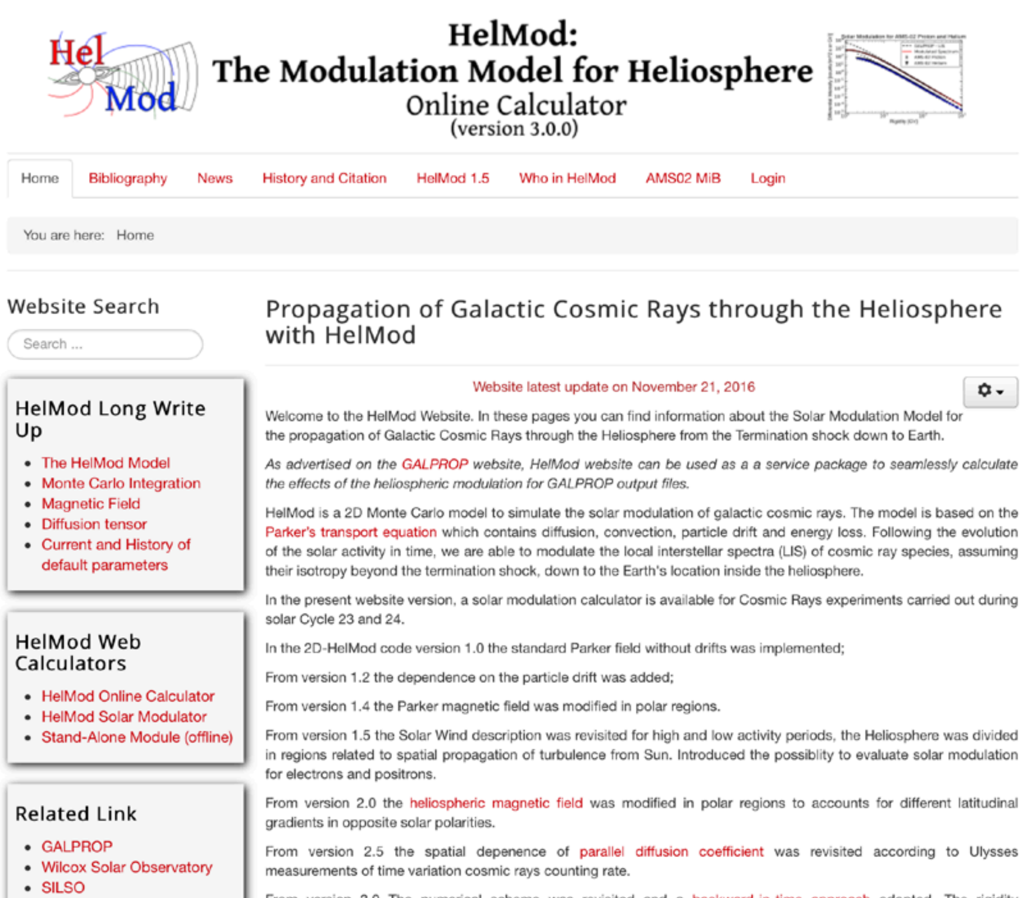

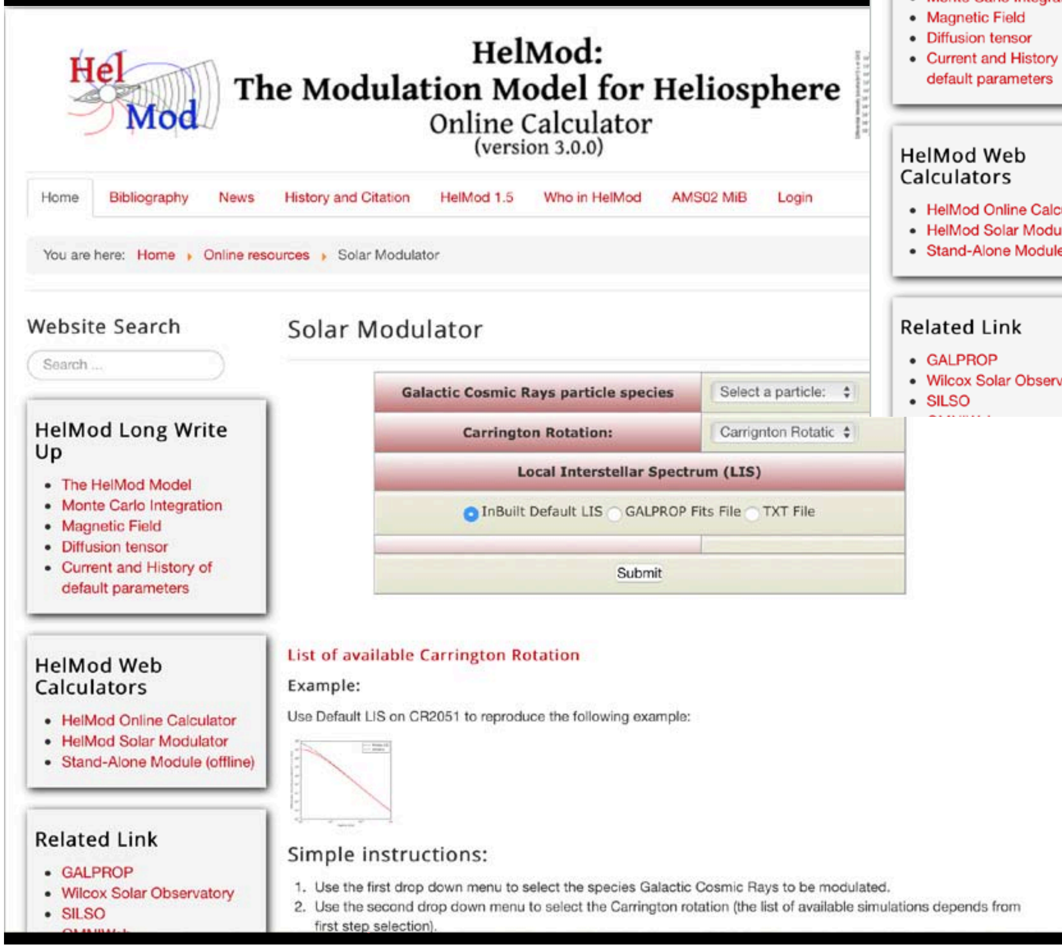

- ✧ Time-dependent Parker (1965) equation
- ✧ 2D Monte Carlo
- ✧ Diffusion, convection, energy losses, general description of the symmetric and antisymmetric parts of the diffusion tensor (charge-sign dependent drift effects)

HelMod vs. Ulysses

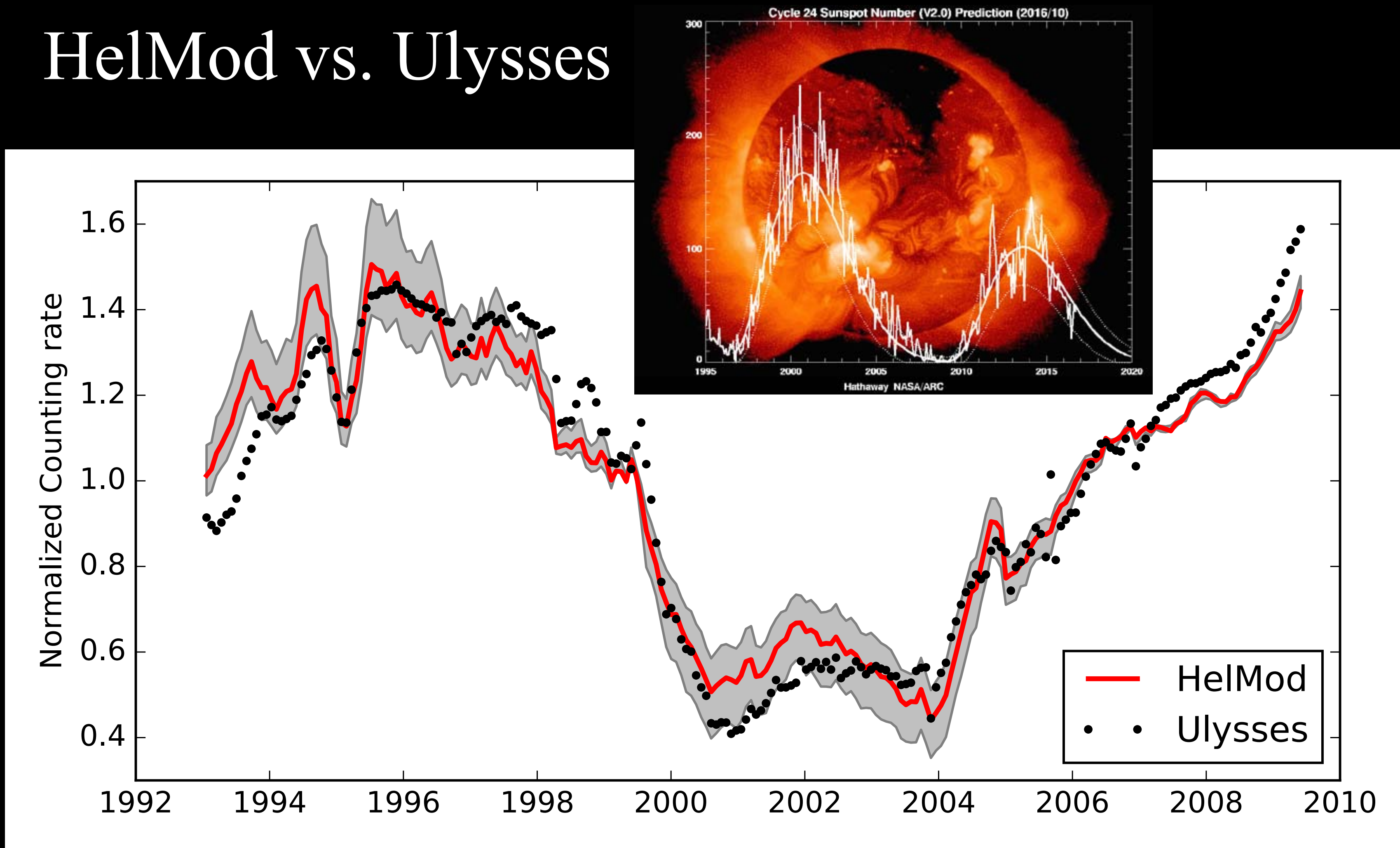

- ✧ Ulysses – outside the ecliptic up to ±80◦ in solar latitude and at ~1–5 AU
- ✧ Ulysses counting rate normalized to the average value for the KET coincidence channel K12 (proton in energy range 0.25-2.2 GeV/nucleon). Solid line is the HelMod result provided for proton at 2.2 GeV for each Carrington rotation.

Solar cycles 23 & 24

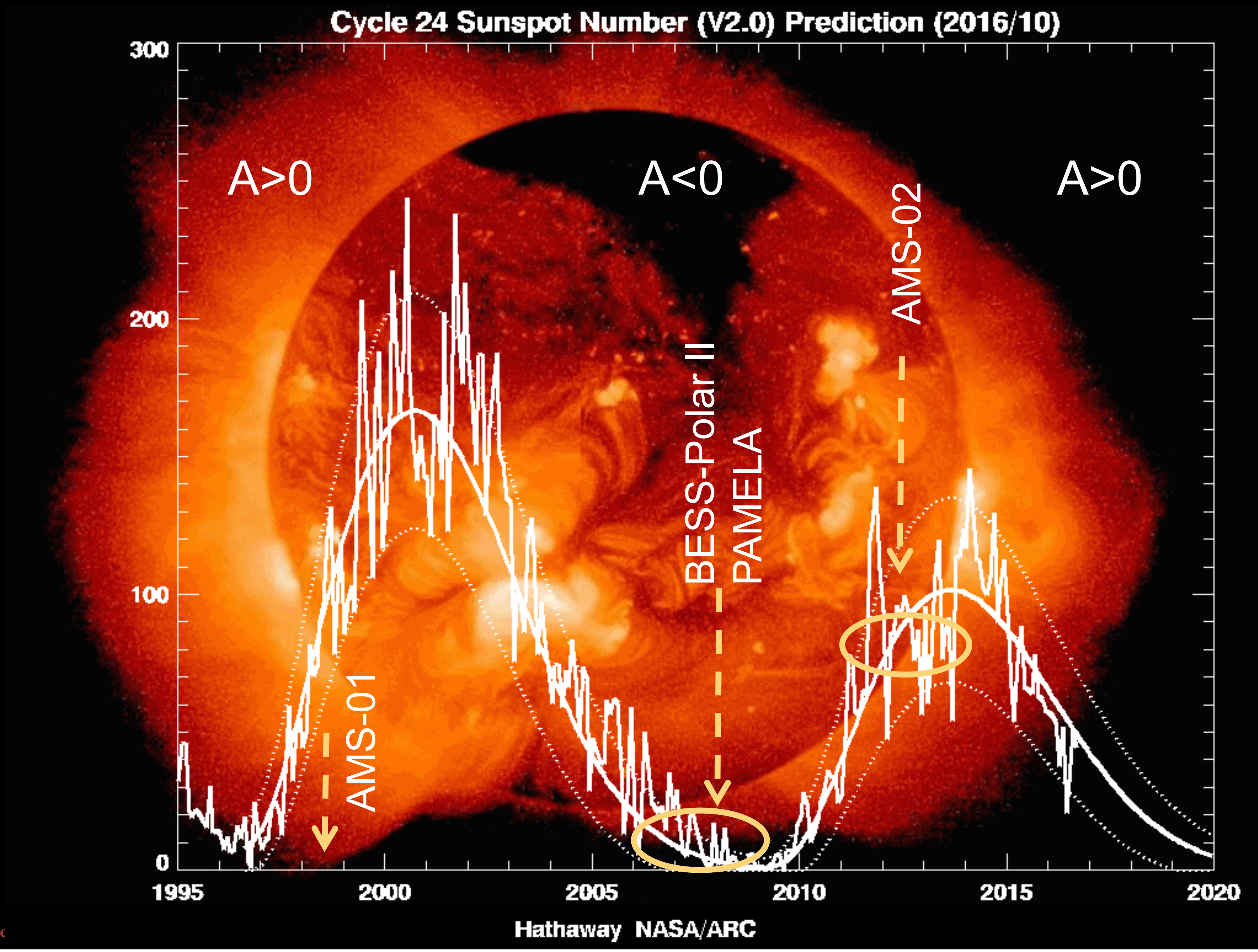

Sourc

Low solar activity (A≳0)

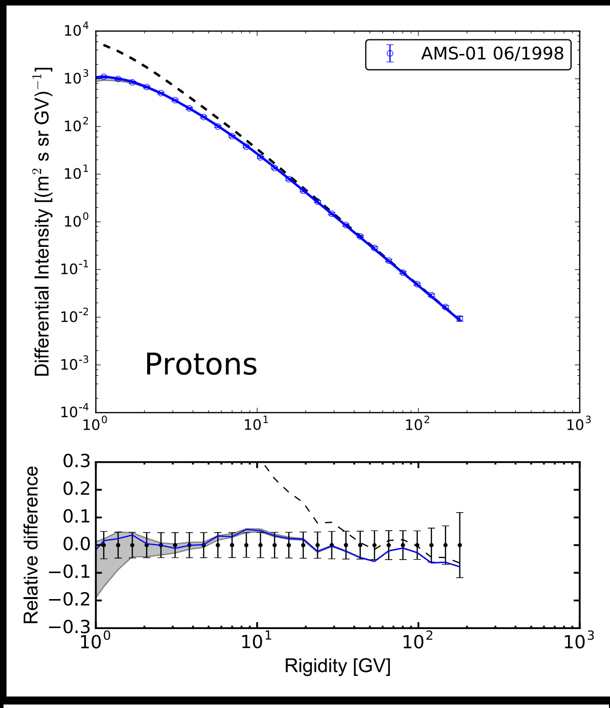

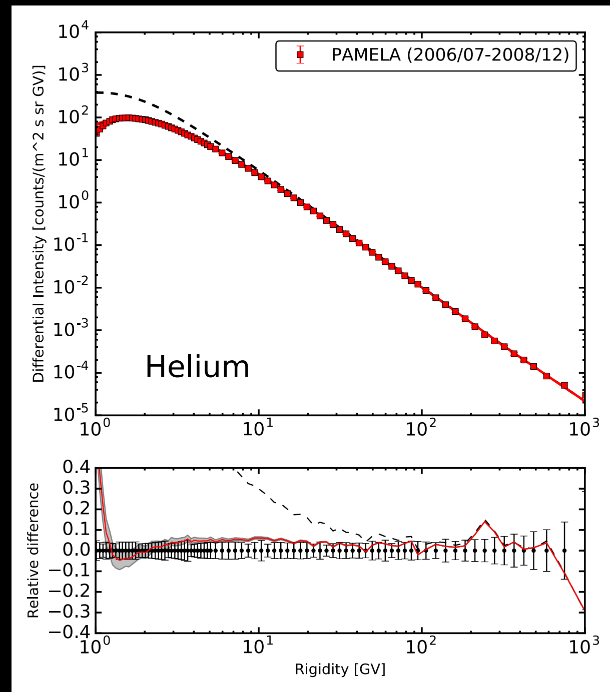

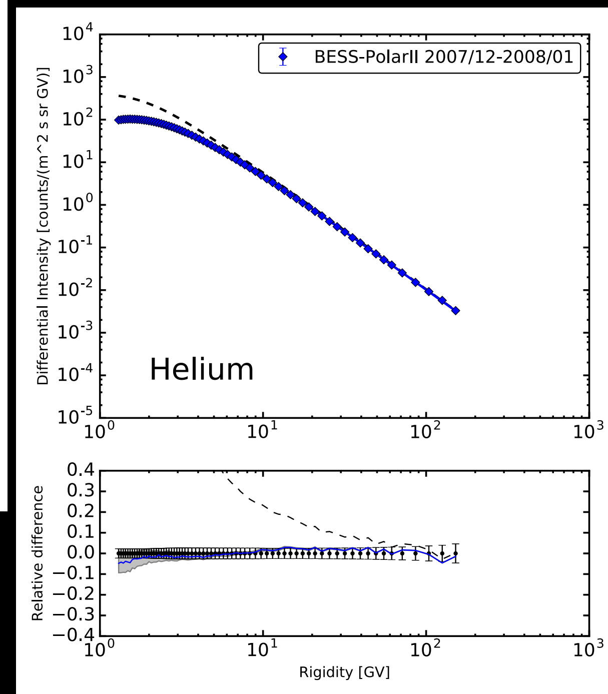

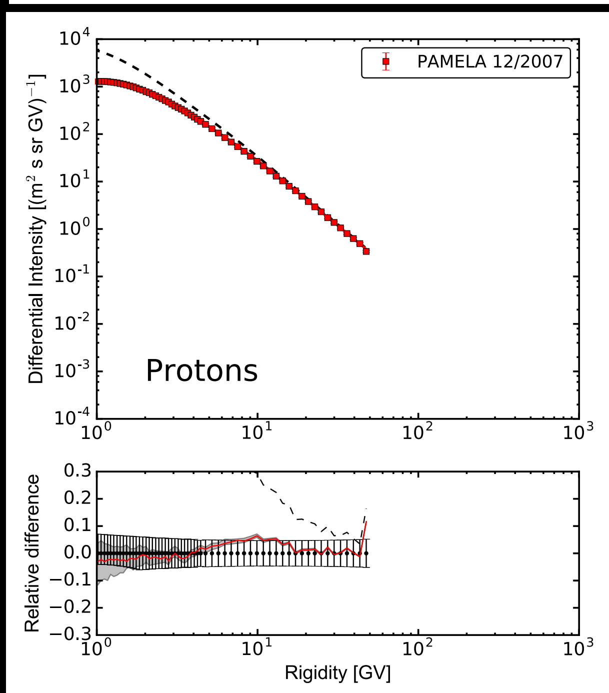

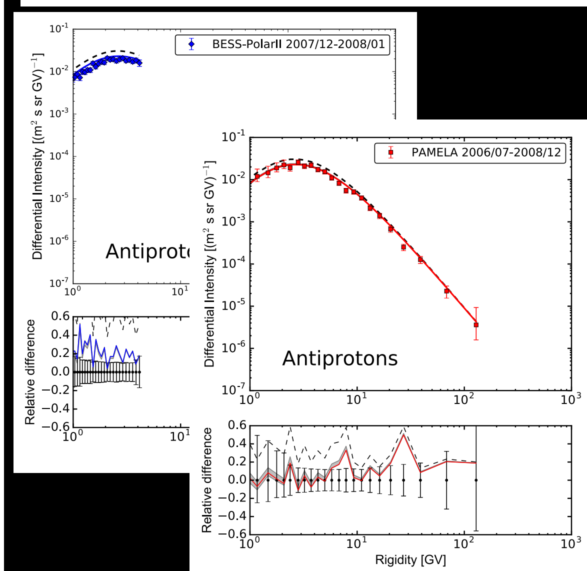

- ✧ GALPROP/HelMod calculations for periods of low solar activity for both polarities of heliospheric magnetic field

High solar activity 2011-15

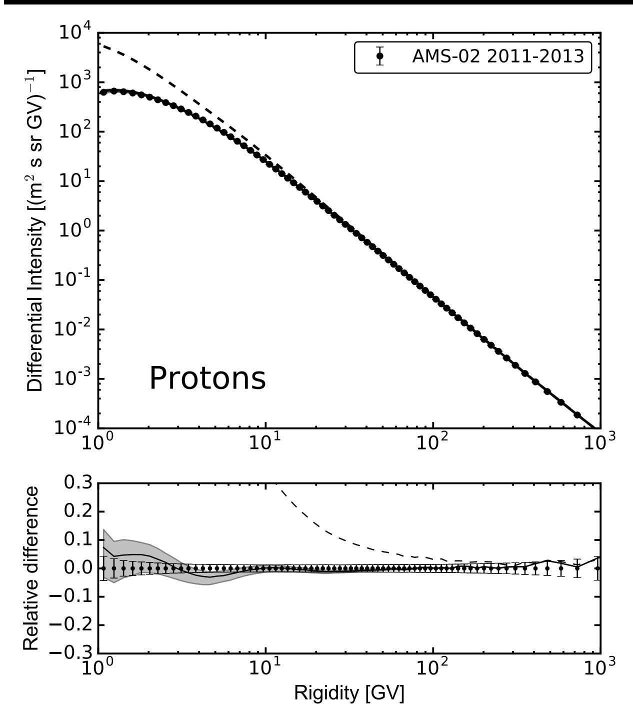

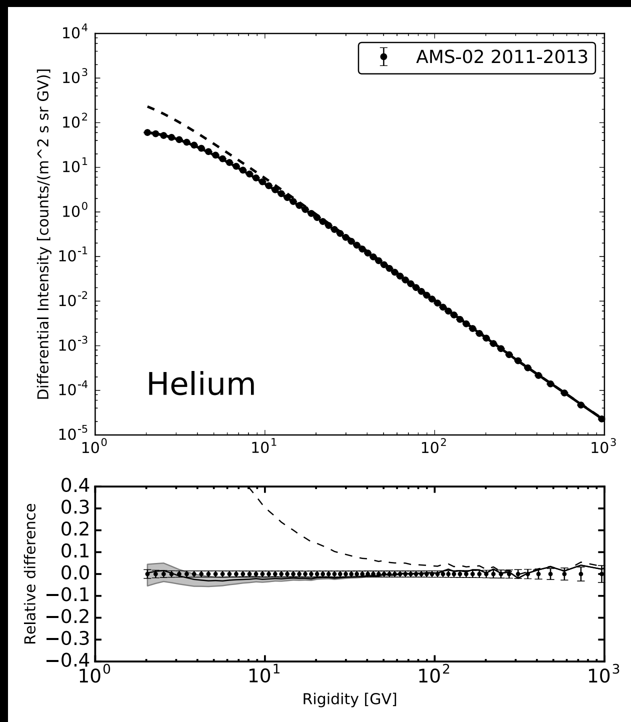

- ✧ AMS-02 data precision – a few %
- ✧ Fitting them with a physical model is a challenge

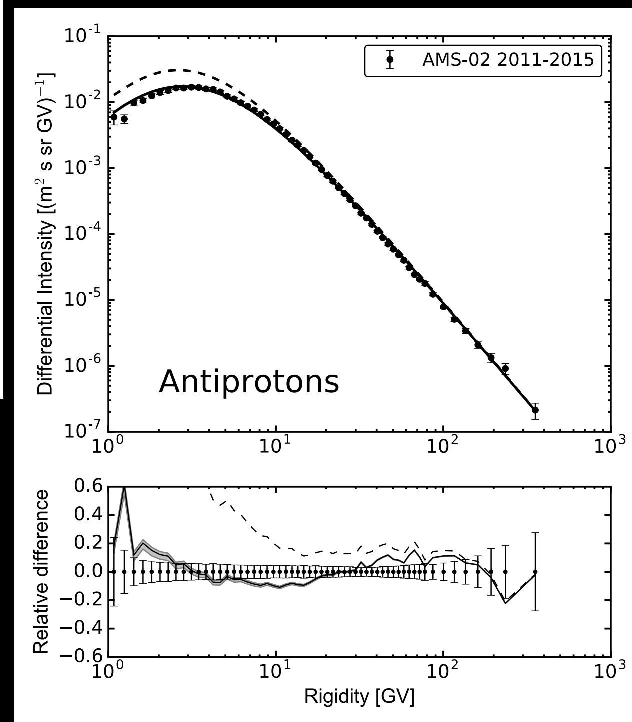

- ✧ GALPROP/HelMod calculations for periods of high solar activity vs AMS-02 data
- ✧ A comparison also made with transitional periods data sets and the agreement is good

Comparison of pbar spectra taken at different epochs

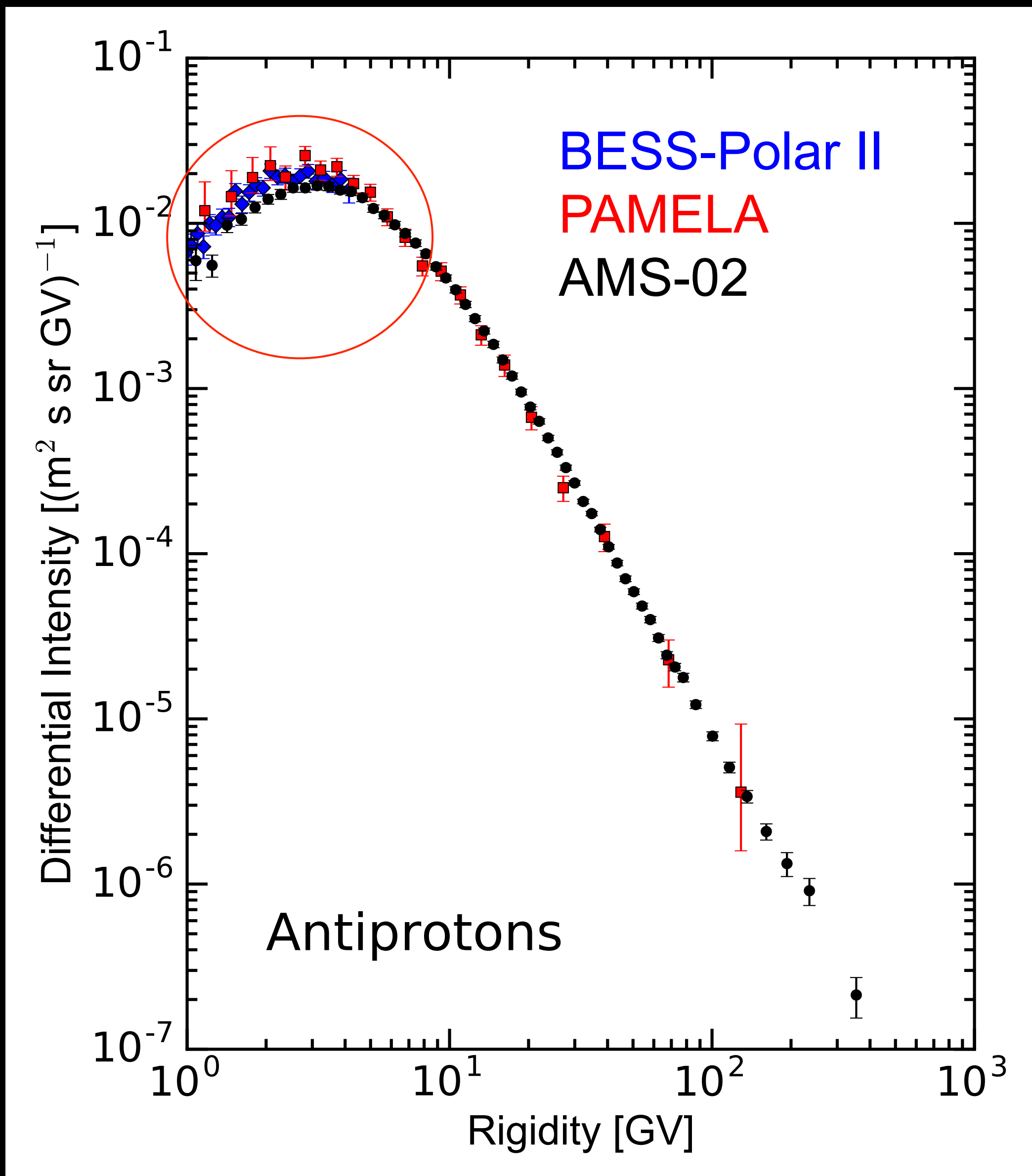

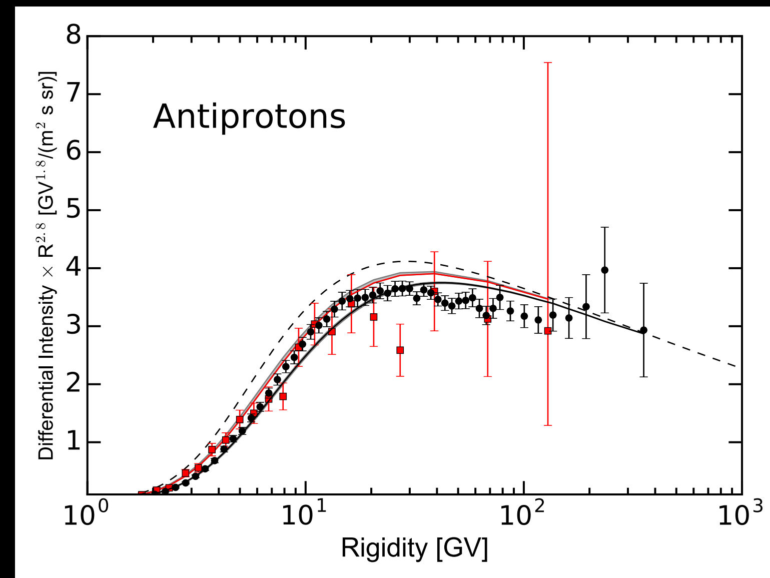

- ✧ BESS-Polar II & PAMELA data are taken at low activity period (A<0) vs AMS-02 at high solar activity period

Bayesian Analysis of CR propagation

- First successful attempt – Trotta+'11
- SuperBayeS with optimized GALPROP
- Statistical analysis of the entire parameter space
- Returns global best fit points and confidence limits
- Includes "nuisance" parameters

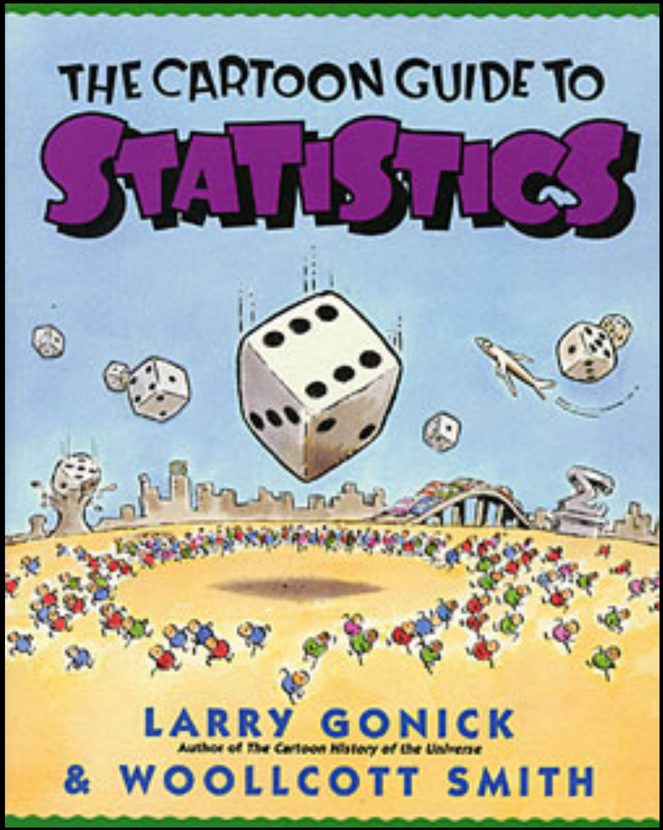

- New analysis (Johannesson+'16) employs machine-learning techniques (BAMBI algorithm), reduces computing time by ~20%
- BAMBI = MultiNest sampling + SkyNet neural network training
- Constrains both CR propagation parameters and source abundances (reacceleration model)
- Split data sets: (i) pbar, p, He and (ii) light nuclei: Be-Si
- Finer grid provides better accuracy

Problems with antiprotons

- GALPROP was used to make accurate calculations of pbars in CR in 2002 and 2003
- Comparison with BESS data
- Problems of reacceleration model at GeV energies – “antiproton excess”

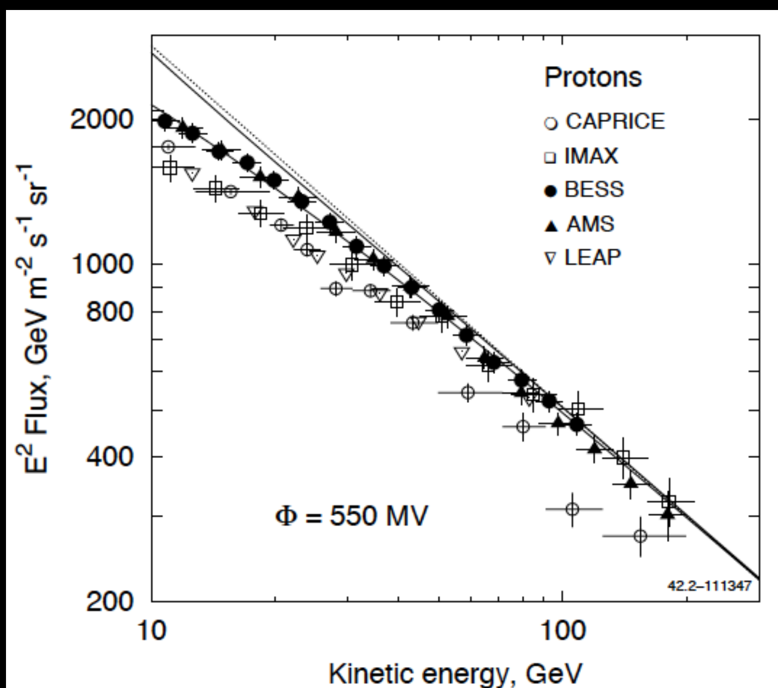

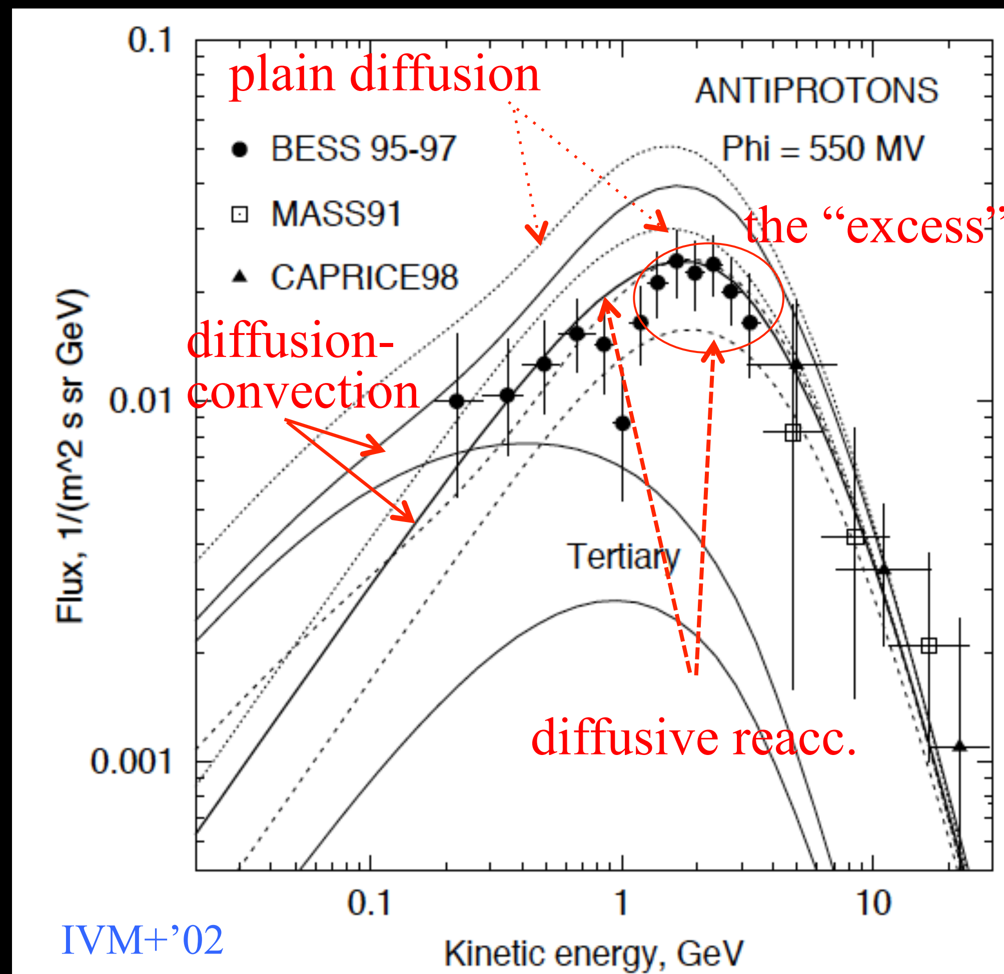

Computational effort

- ✧ pbar, p, He scan
  - 144 CPUs
  - 2M GALPROP calls
  - 5.5 CPU years
- ✧ Be-Si scan
  - Iterative procedure
  - 96 CPUs
  - 2M GALPROP calls
  - 35 CPU years
- ✧ BAMBI efficiency
  - 1% effort spent on training
  - saved 20%: ~10 CPU years or 4.5 months of real time

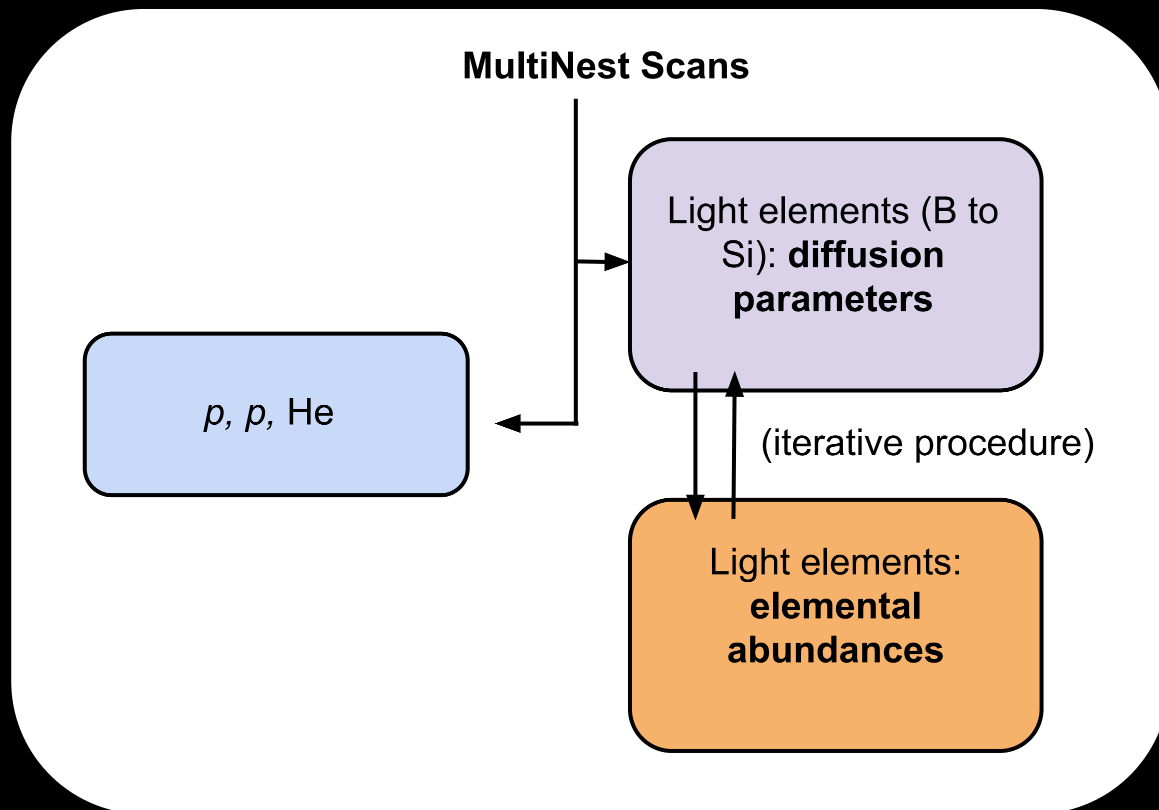

Johanneson+'16

Light element scan

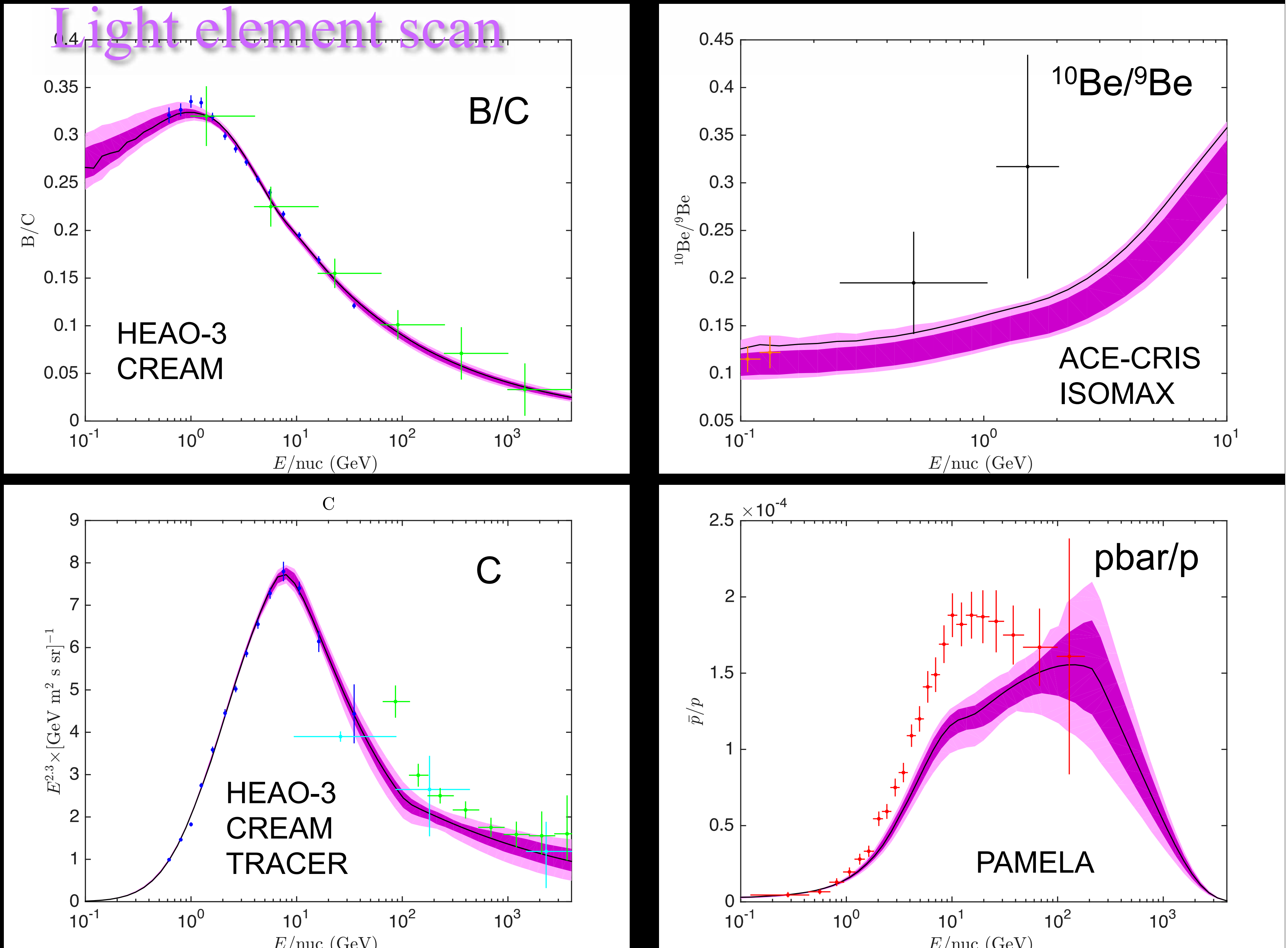

pbar, p, He scan

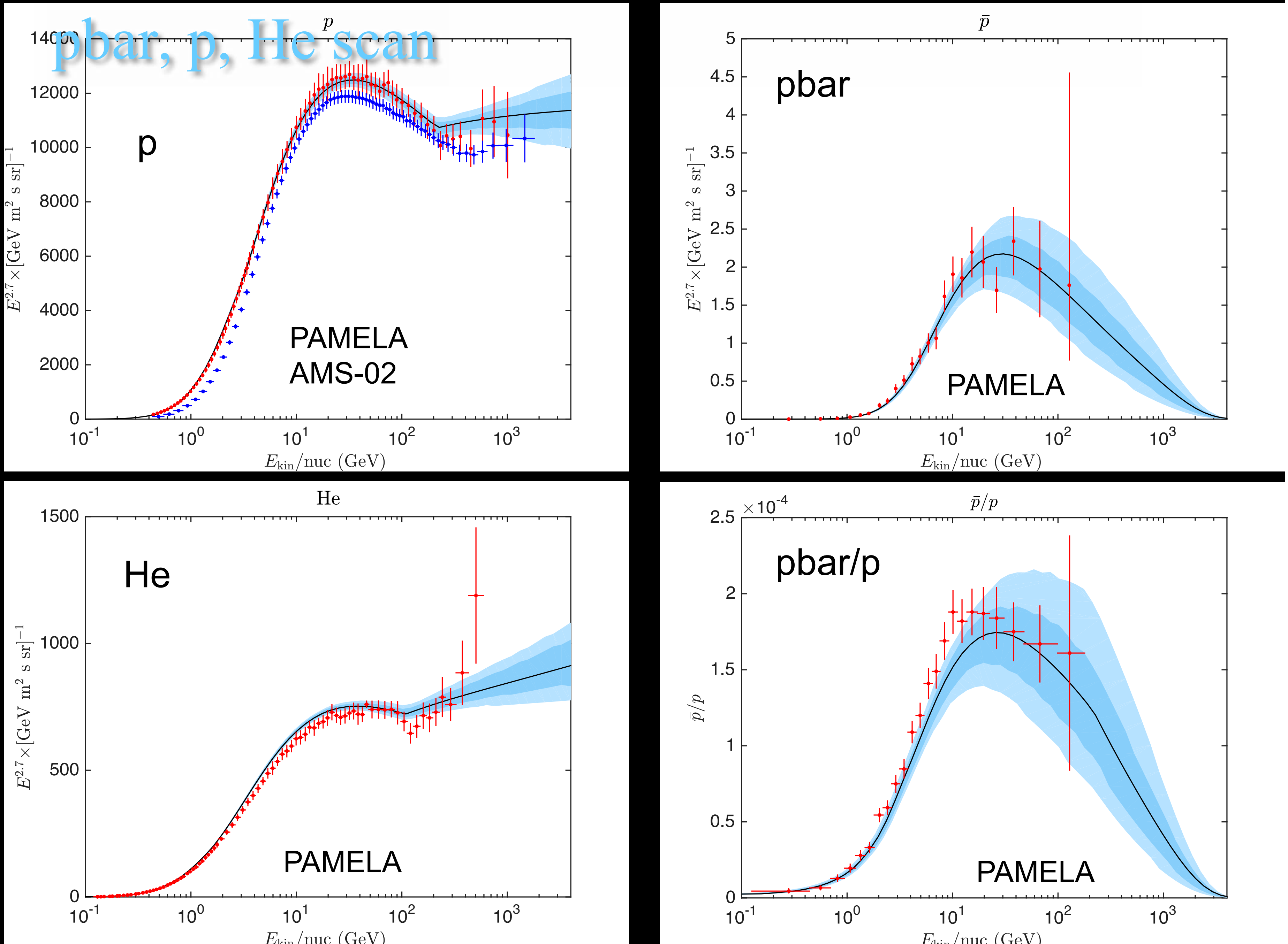

2D posterior distributions

- 2D posterior distributions:
  - halo size z_h vs diffusion coefficient D_0
  - Alfven velocity v_{Alf} vs diffusion coefficient D_0
- Clearly demonstrate the distributions do not overlap
- Interpretations:
  - Non-uniform diffusion coefficient in the Galaxy
  - Local sources (~1 kpc) of primary nuclei (IVM+'03, Shaviv+'09)

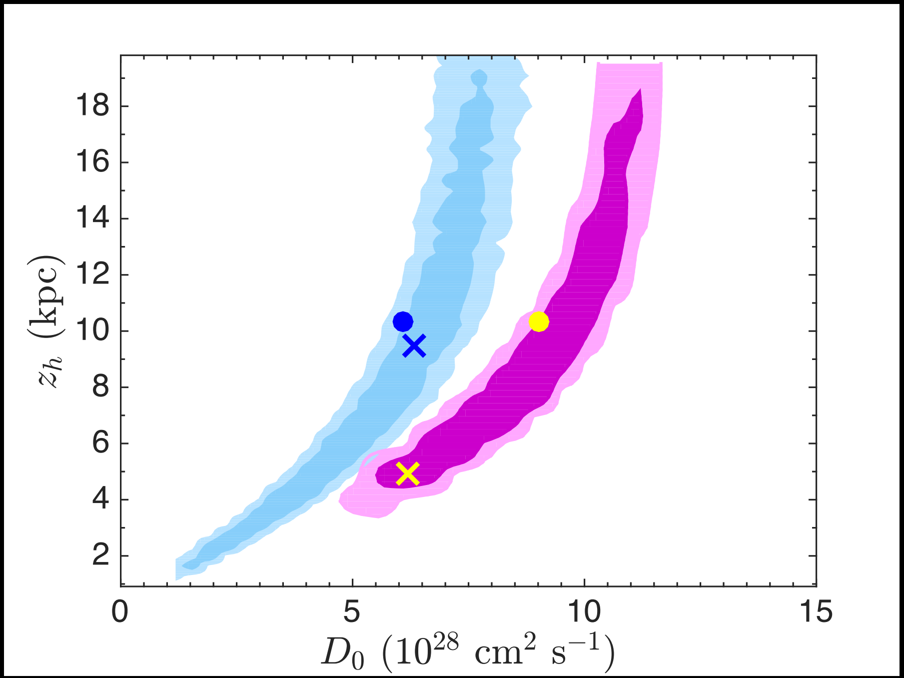

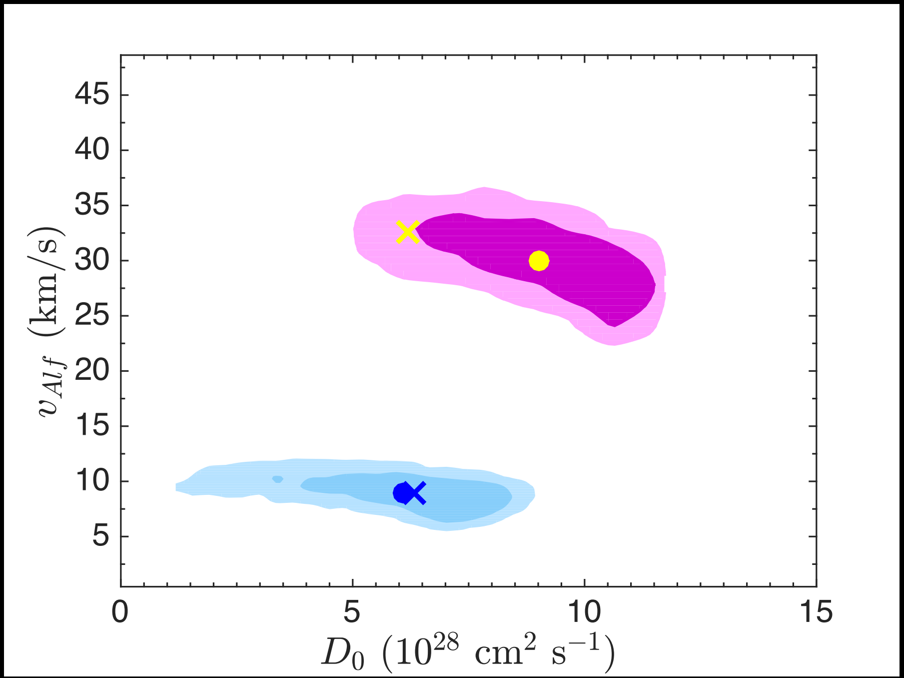

Non-uniform diffusion

- Interaction time scale

$$\tau \sim [\sigma_r n c]^{-1}$$

- Diffusion coefficient

$$D_{xx} = \beta D_0 \left(\frac{\rho}{\rho_0}\right)^{\delta}$$

- Effective propagation distance

$$\langle x \rangle \sim \sqrt{6D\tau} \sim \left(\frac{6D_0}{\sigma_r n c}\right)^{1/2} \left(\frac{\rho}{\rho_0}\right)^{\delta/2}$$

- Total inelastic cross section (fragmentation) at a few GeV/nuc

$$\sigma_r(A) \approx 250 \text{ mb } (A/12)^{2/3}$$

- p, pbar inelastic cross section ~40 mb

- Effective propagation distance of carbon nuclei and protons (antiprotons)

$$\langle x \rangle_A \sim 2.7 \text{ kpc } \left(\frac{A}{12}\right)^{-1/3} \left(\frac{\rho}{\rho_0}\right)^{\delta/2}$$

$$\langle x \rangle_p \sim 5.6 \text{ kpc } \left(\frac{\rho}{\rho_0}\right)^{\delta/2}$$

$\rho_0 = 4$ GV

- Probes the area ~ $< x >^2$: p probes 4 times the area that is probed by C

Total inelastic cross sections C-Zn

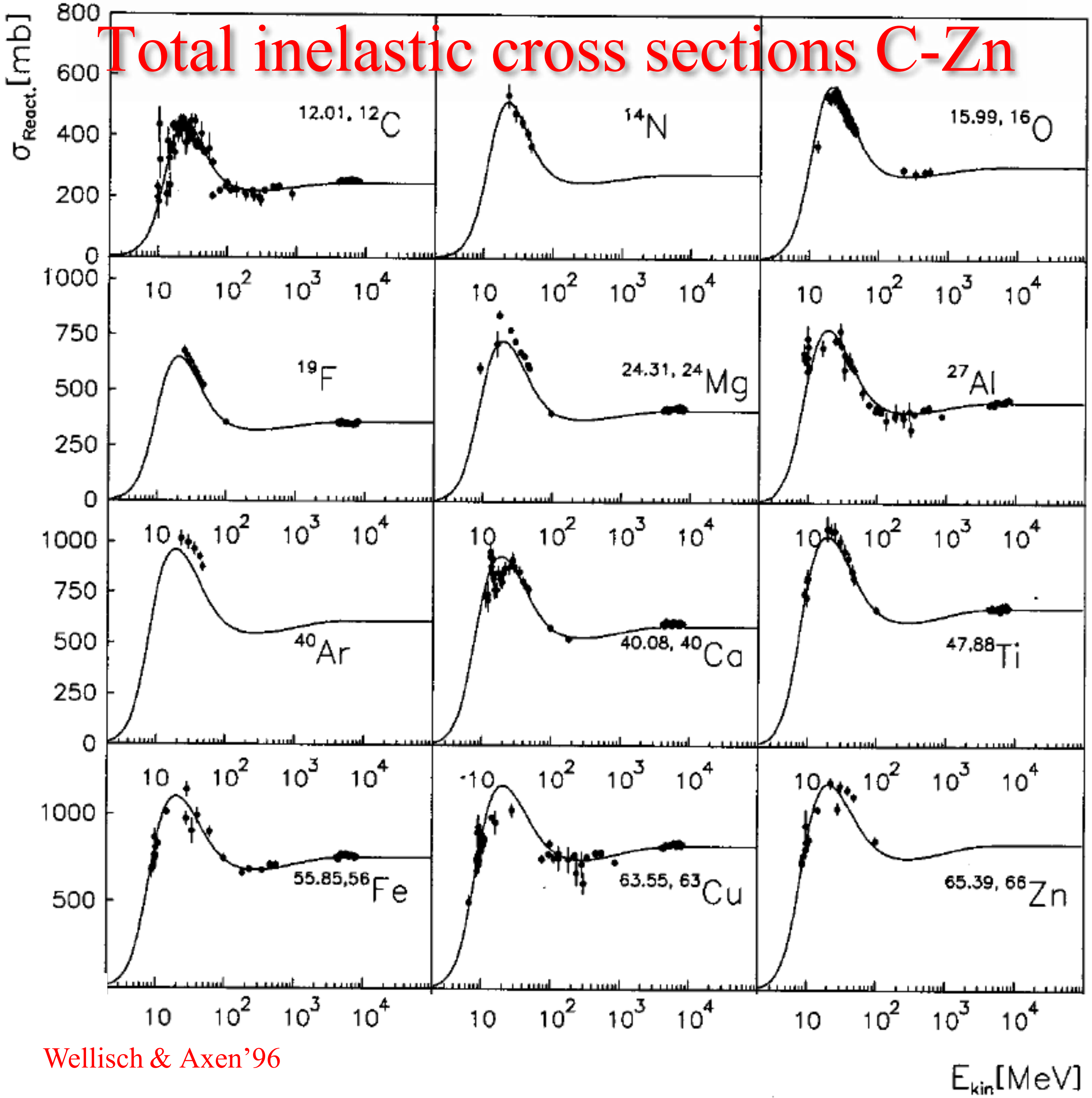

Wellisch & Axen'96

Above ~1 GeV/n:

$\sigma \sim 250$ mb $(A/12)^{2/3}$

Total inelastic cross sections Fe-U

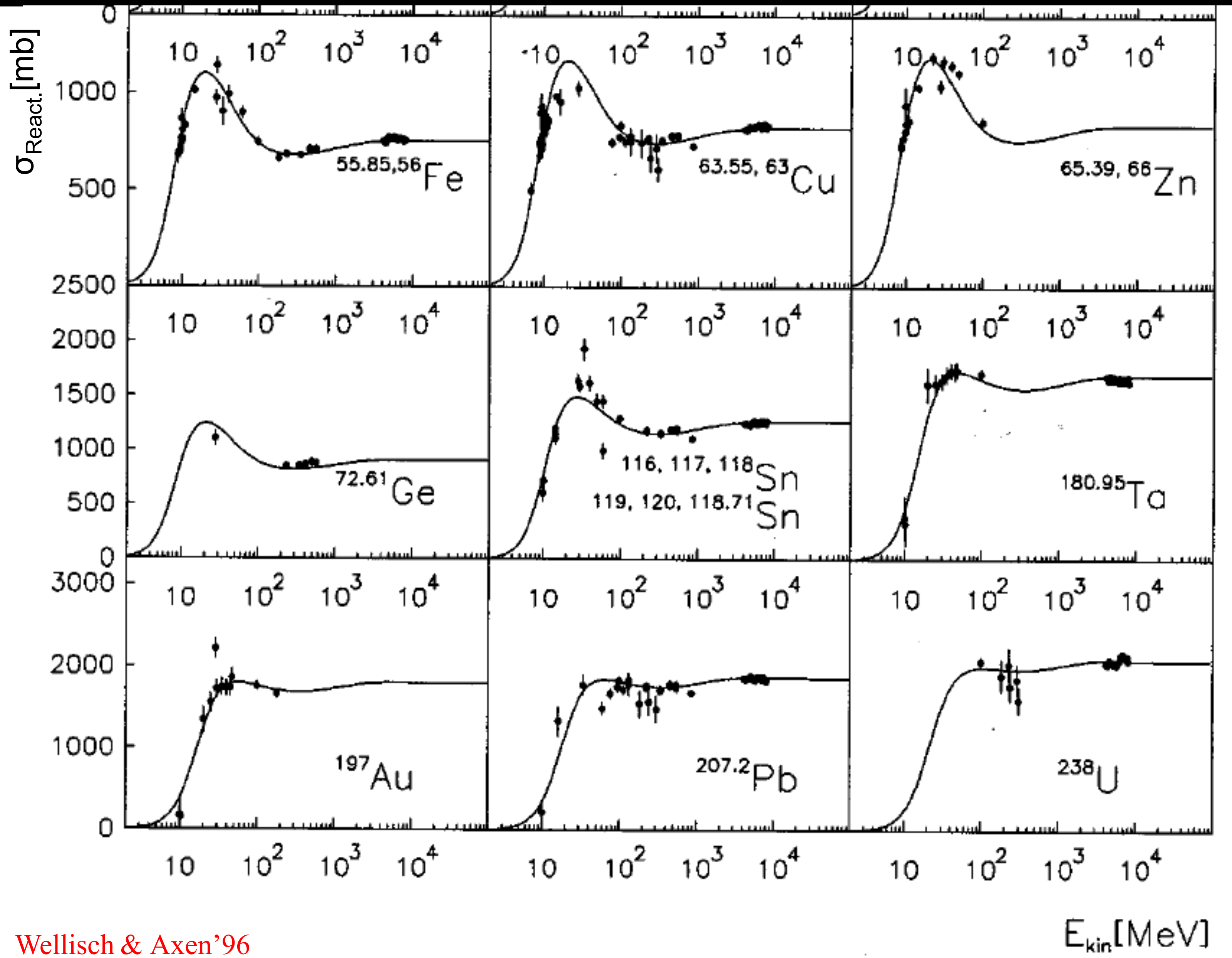

Wellisch & Axen'96

Direct probes of CR propagation

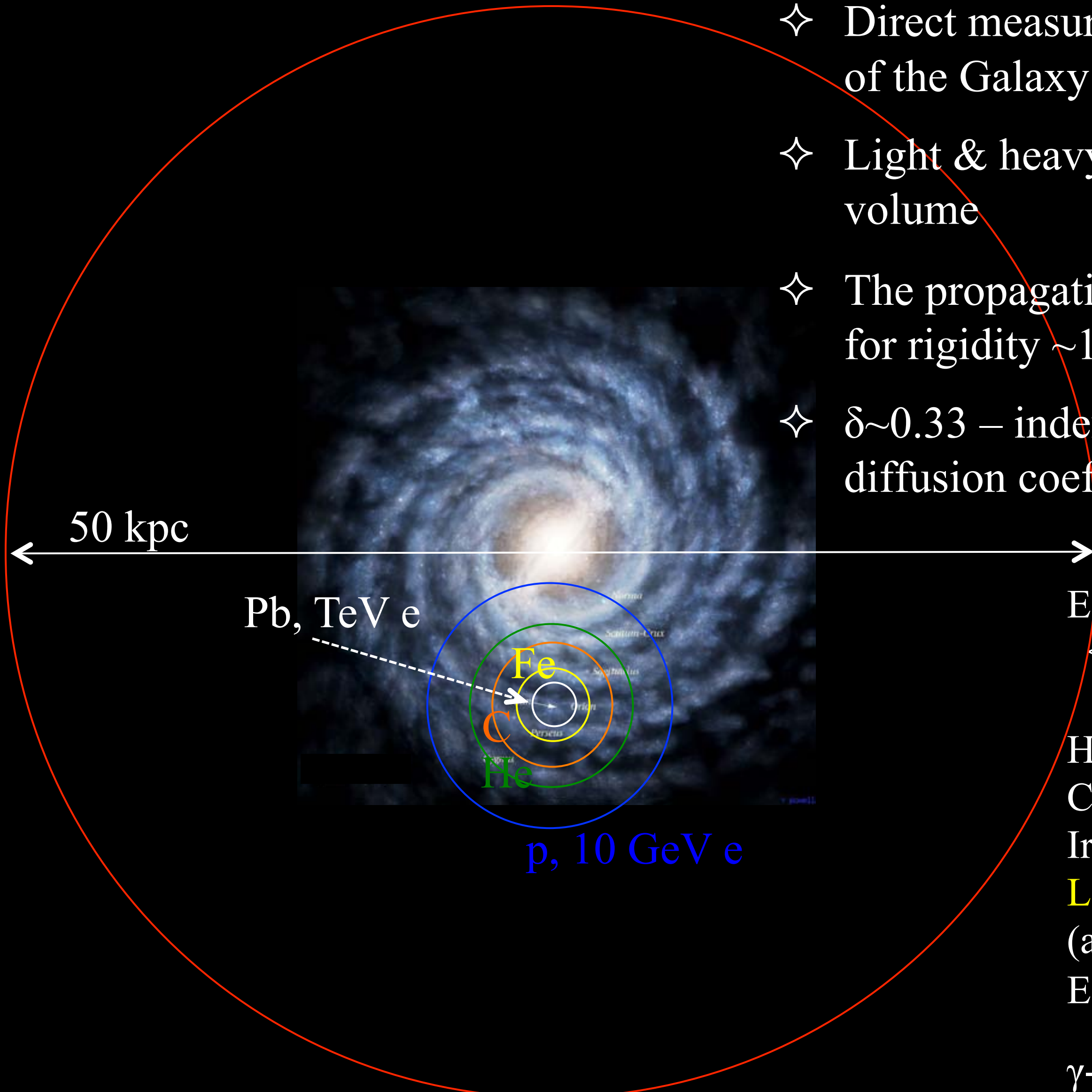

- Direct measurements probe a very small volume of the Galaxy
- Light & heavy nuclei probe different propagation volume
- The propagation distances are shown for nuclei for rigidity ~1 GV, and for electrons ~1 TeV
- $\delta \sim 0.33$ – index of the rigidity dependence of the diffusion coefficient

Effective propagation distance:

$\langle X \rangle \sim \sqrt{6D\tau} \sim 2.7 \text{ kpc } R^{\delta/2} (A/12)^{-1/3}$

Helium: ~ 3.6 kpc $R^{\delta/2}$
Carbon: ~ 2.7 kpc $R^{\delta/2}$
Iron: ~ 1.6 kpc $R^{\delta/2}$
Lead ~ 1.0 kpc $R^{\delta/2}$
(anti-) protons: ~ 5.6 kpc $R^{\delta/2}$
Electrons ~ 1 kpc $E_{12}^{-\delta/2}$

γ-rays: probe CR p (pbar) and e± spectra in the whole Galaxy ~50 kpc across


What's next?

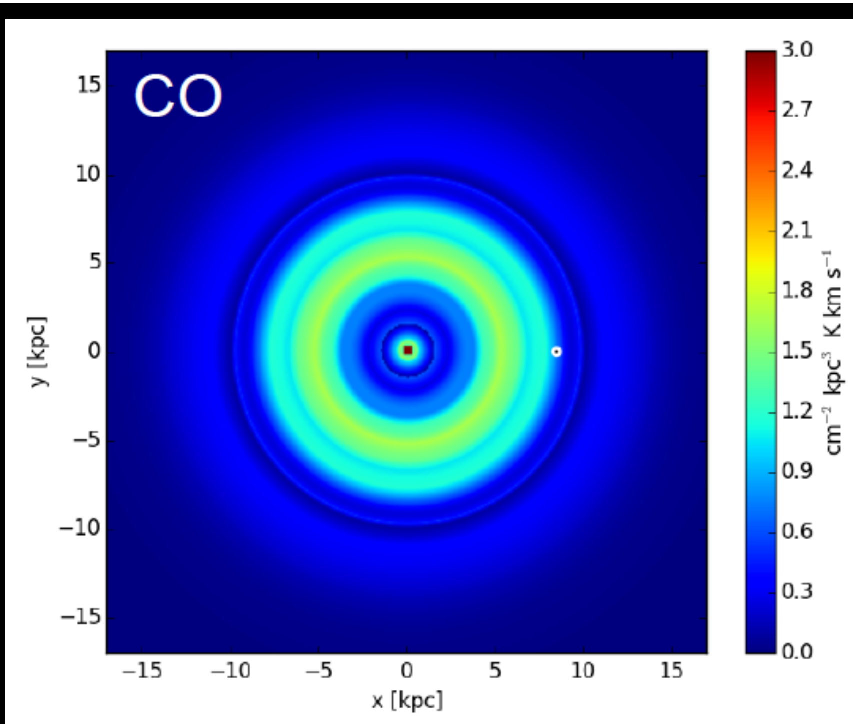

2D Galaxy: surface density

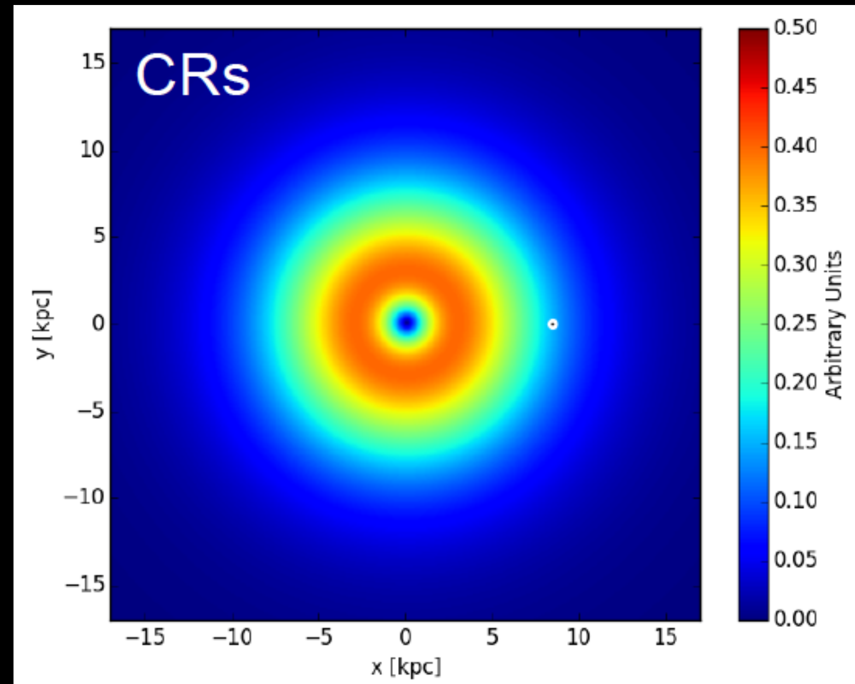

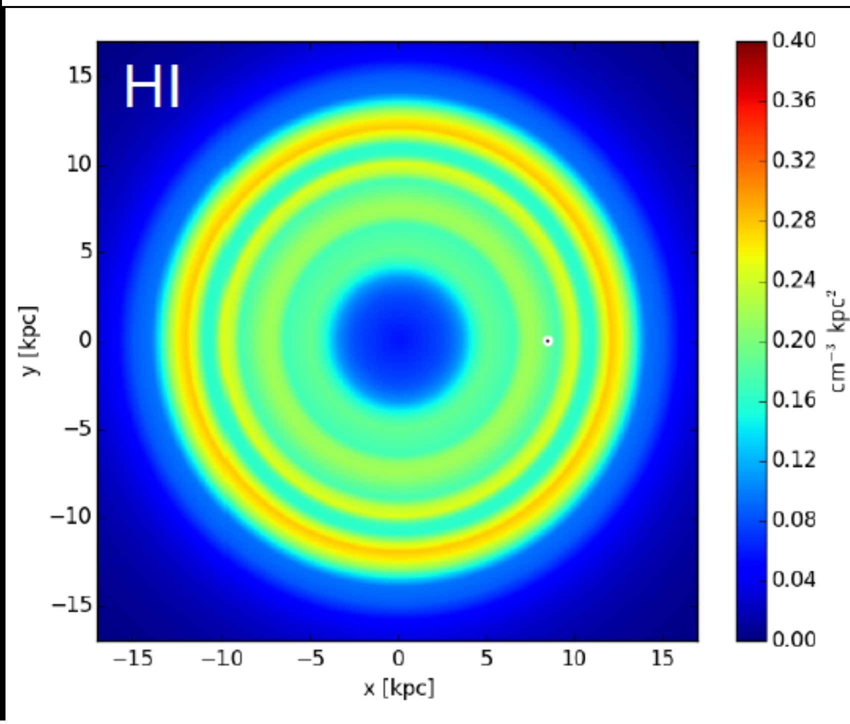

- ✧ Currently used in GALPROP: Cylindrically symmetrical distributions of the gas components and CRs

3D Galaxy: surface density

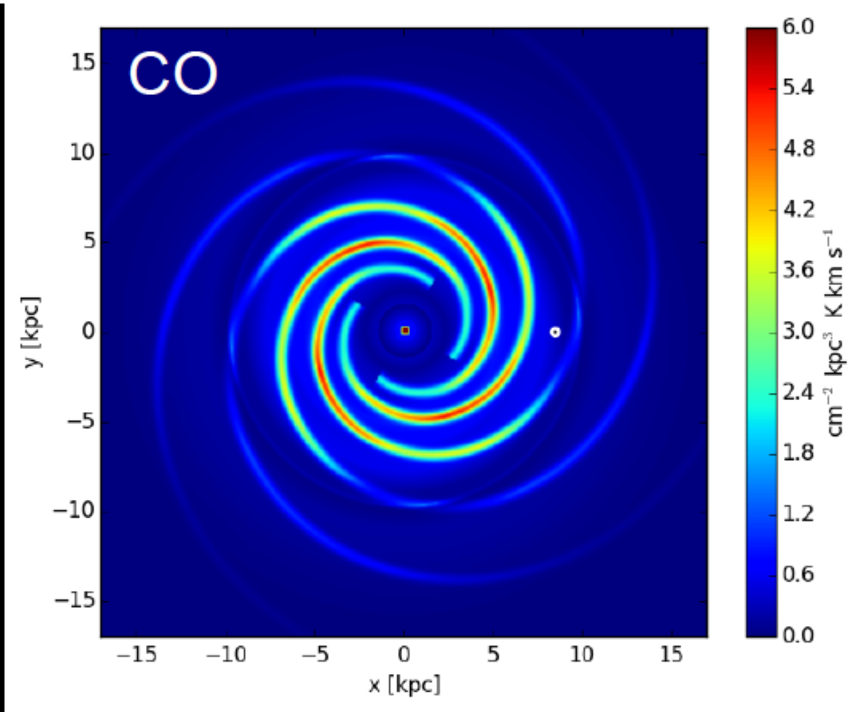

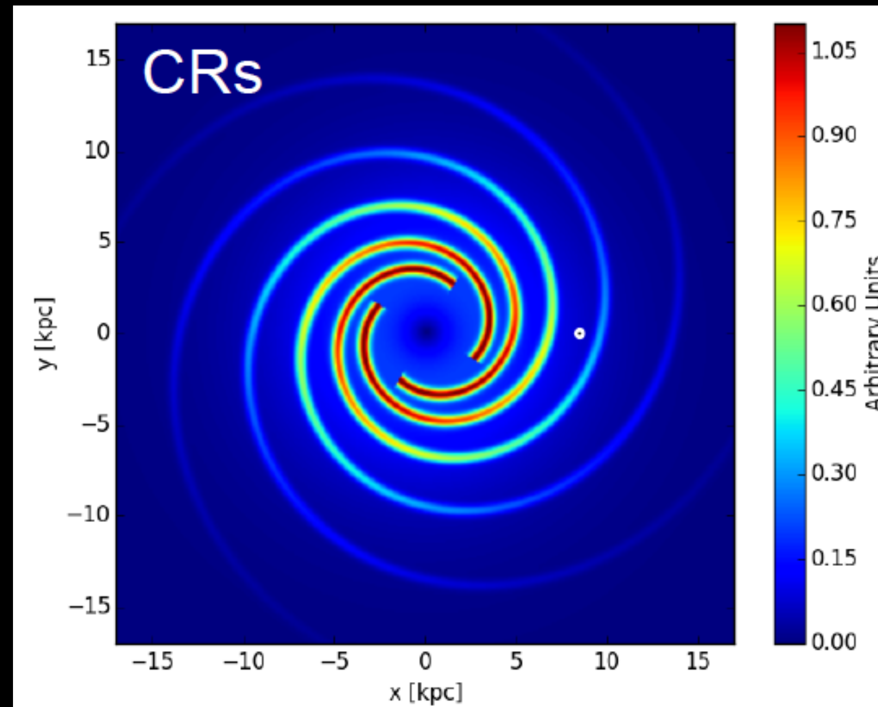

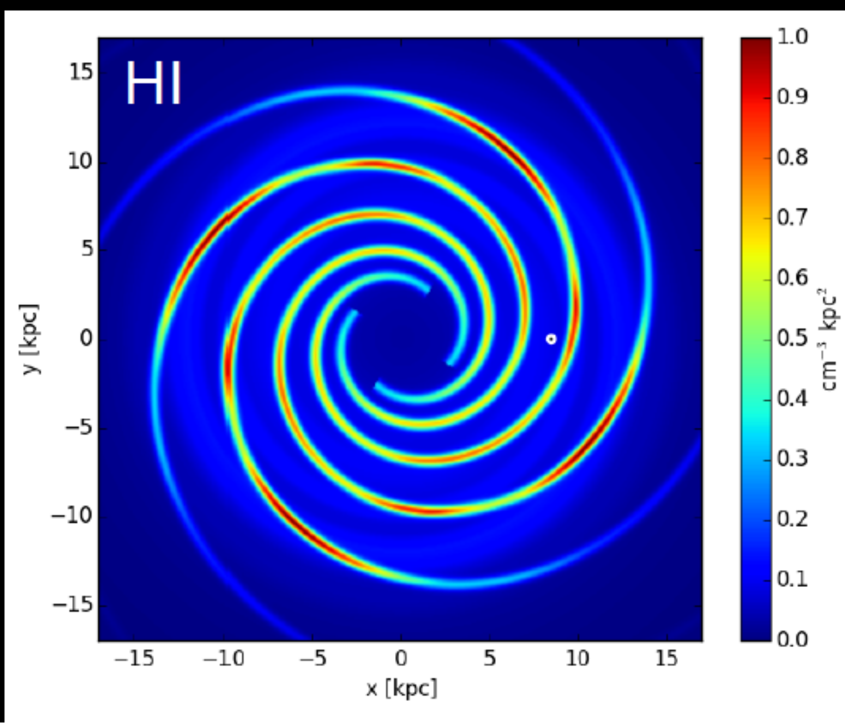

✧ One of the model realizations: ~50% gas in the spiral arms

Johannesson+'15 (GALPROP)

Effects of the 3D spiral structure

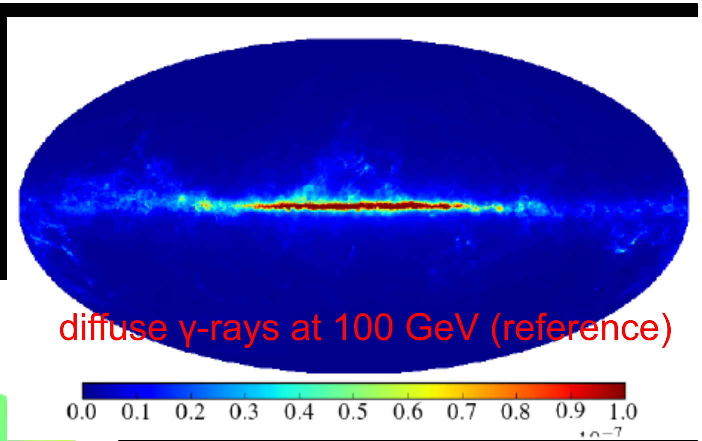

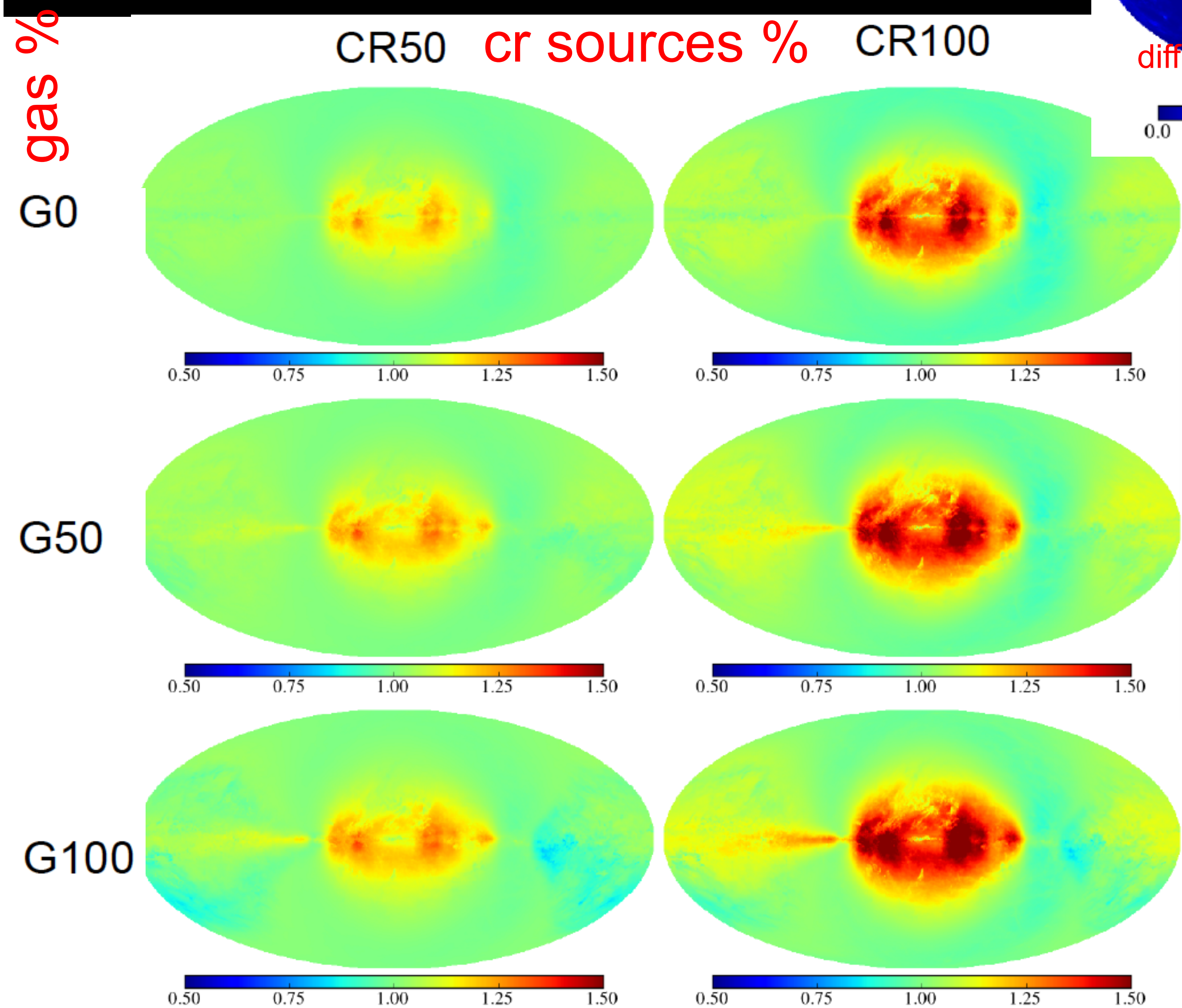

- ✧ The 3D/2D skymap ratios
- ✧ Strong effects in the inner Galaxy, tangentials to the spiral arms, and in the plane

3D radiation field

- ✧ Surface map shows the elements of the Galactic structure included in the 3D model
- ✧ Inverse Compton subtraction map (3D-2D) at 12 GeV

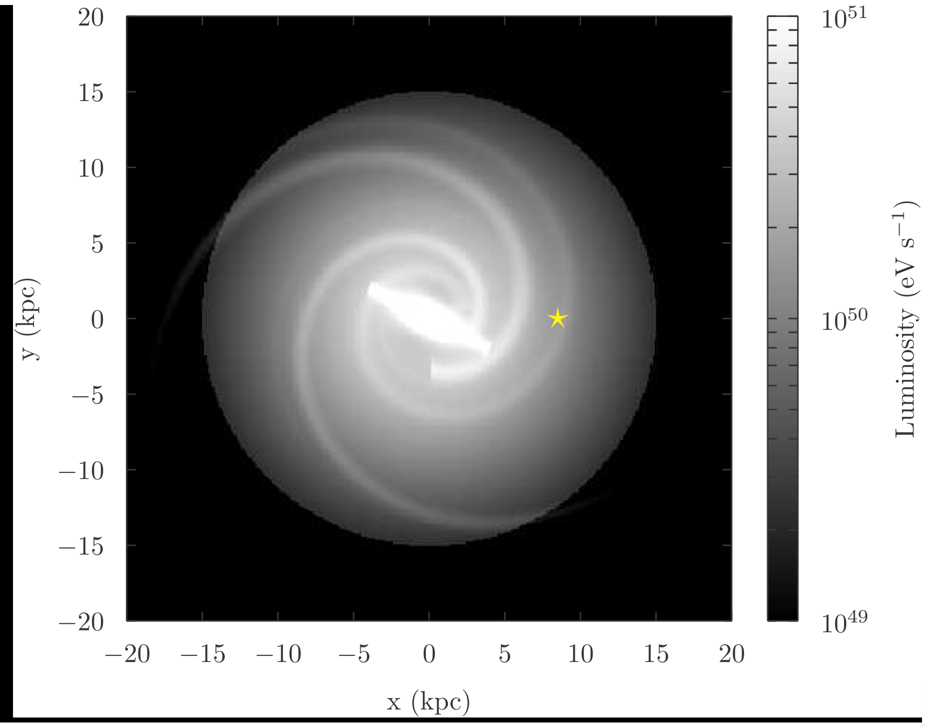

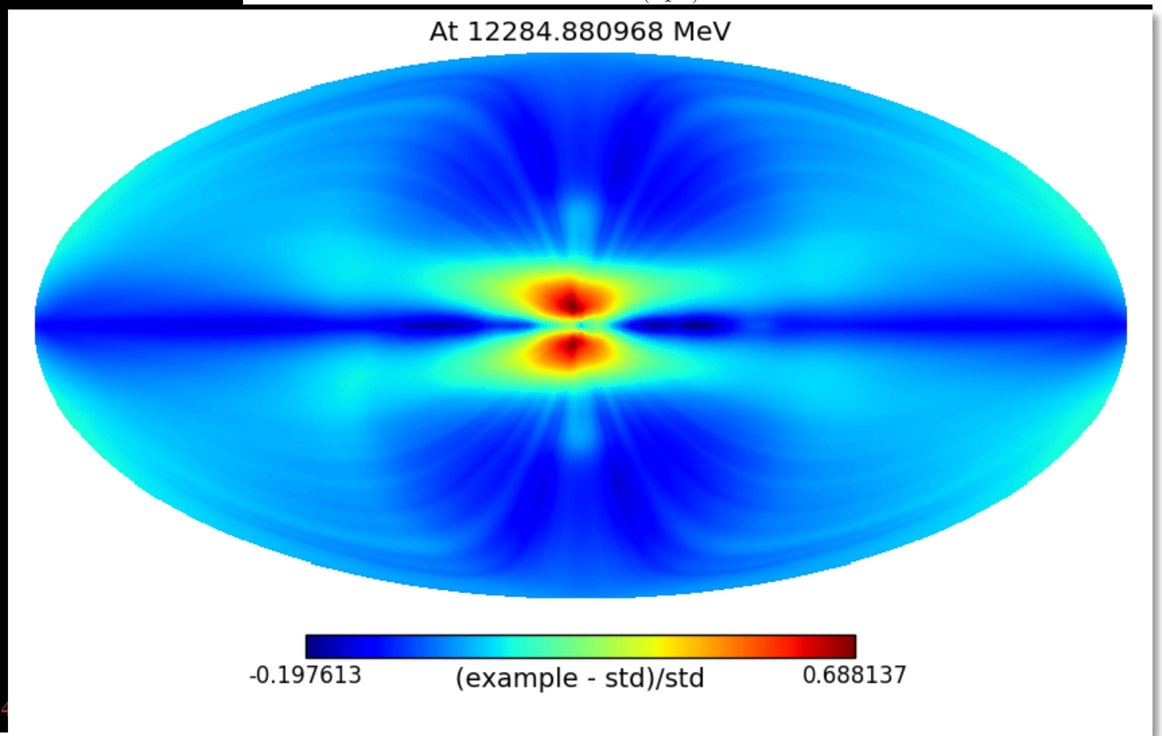

Porter+'15


Et voilà, j'ai fini.
Merci beaucoup.